Formation of Polyelectrolyte Nanocapsules for Drug Release Induced by Ultrasonic Stimulation

Thesis submitted by

Yan Bao

Department of Biomedical Engineering

University of Strathclyde

This thesis is submitted in partial fulfillment of the requirements for the

Degree of Master of Philosophy in Biomedical Engineering

July 2016

Declaration of Work

This thesis is the result of the author's original research. It has been composed by the author and has not been previously submitted for examination, which has led to the award of a degree.

Signed:

Date:

Acknowledgements

I want to present my sincere thanks to Dr. Wei Yao, my supervisor. I would not be able to have completed this project without his patient guidance and constructive suggestions.

Also, I am grateful to my classmates, friends, and staffs in biomedical engineer department, such as Pae, Riduan, and Sarah for their help and discussion. In physics department, some members gave me a great deal of help on experimental operation requirements. I want to thank Dr. Yu Chen sincerely for her expertise and suggestions in this research. In the research group of photophysics, members such as Peng Gu, Qingjiang Xue, gave me assistance in my research. In the gold nanoparticles synthesis, their experience and advice are valuable for the trouble shooting of my experiments. Their experience was inspiring for my graduate study.

I would like to thank my parents for their care, support and love. With their encouragement and support, I have more confidence in facing challenges in my life.

Abstract

This thesis investigates the drug release from polymeric nanocapsules induced by ultrasonic stimulation. A drug delivery system with stimuli-responsive polymeric nanocapsules was prepared to achieve locally controlled drug release by remote ultrasonic stimulation. This was then compared to the polymeric capsules for spontaneous drug release. Nanocapsules were produced by employing a layer-by-layer technique, encapsulated with Rhodamine 6G dye used in place of anti-restenotic drugs. Ultrasonic stimulation induced dye release was monitored by fluorescence intensity changes in the fluorescence emission spectra taken from the supernatant of the nanocapsule solutions after ultrasonic treatment. Gold nanoparticles were incorporated in the shell of the nanocapsules. The presence of gold nanoparticles significantly enhanced the efficiency of the ultrasonically induced dye release from the nanocapsules and increased the sensitivity of the nanocapsules to ultrasonic stimulation compared to those without gold nanoparticles.

Table of Contents

List of Abbreviations

AuNPs	Gold nanoparticles
CAD	Coronary artery disease
CVD	Cardiovascular disease
DES	Drug-eluting stent
EVAL	Ethylene-vinyl alcohol
GSH	Glutathione
ib-PEI	2-iminobiotin-labeled poly(ethyleneimine)
IR	Infrared radiation
ISR	In-stent restenosis
LbL	Layer-by-layer
mTOR	Mammalian target of rapamycin
NIR	Near-infrared radiation
PAA	Poly(acrylic acid)
PAH	Poly(allylamine hydrochloride)
PDDA	Poly(dimethyldiallyl ammonium chloride)
PEG	Poly(ethylene glycol)
PEI	Poly(ethyleneimine)
PEM	Polyelectrolyte multilayer
PEO-b-PPO-b-PEO	Poly(ethylene oxide)-block-poly(propylene oxide)-block-poly(ethylene oxide)

PHEMA	Poly(2-hydroxyethyl methacrylate)
PLA	Polylactic acid
PSS	Poly(styrene sulfonate)
SEM	Scanning electron microscope
SMC	Smooth muscle cell
SPR	Surface plasmon resonance

List of Figures

Chapter 1: Introduction

1.1 General introduction

The synthesis of nanocapsules with multiple functions for drug delivery systems and a means of external stimulation employed on the nanaocapsules is significant [1]. Due to unhealthy lifestyles and high pressure at work, people are facing a variety of health problems, both physically and mentally. As reported by the World Health Organization, coronary artery diseases (CADs) are some of the most typical cardiovascular diseases (CVDs), resulting in more than 7 million deaths annually in the world [2]. Stent implantation is a commonly used treatment for CADs. However, in-stent restenosis (ISR) remains a serious problem following implantation. The major cause of ISR is the injured arterial wall causing smooth muscle cell (SMC) proliferation and scar tissue accumulation [3]. Anti-restenotic drugs release from stents happens spontaneously after implantation and often is uncontrolled [4]. To cope with this problem, nanocapsules combined with a drug delivery system can enable drug release in a specific site, as required [5-7]. Stimuli-responsive nanocapsules can release the drug in a controlled manner and the non-invasive nature of the technique has advantages in therapeutic applications, such as reduced possibility of infection, avoiding damage to surrounding tissues by devices.

The ideal coupling interaction between the nanocapsule layers and the mode of stimulation needs to be considered. A stimuli-responsive polymer can respond to surrounding environmental factors and induce the release of drugs from the polymer capsules. Stimuli-responsive polymers such as micelle-forming polymer and liposomes-forming polymer can be sensitive to many factors including physical, chemical or biomedical stimulation. Ultrasound, pH, temperature, magnetic fields, and the intensity of light in the microenvironment can induce responses in different ways. The responses can be changes in shape (mostly in shape memory polymers), permeability, and colour. While such changes occurring in the environment are small,

it is enough to stimulate key changes in the unique properties of polymers.

In the current work, ultrasound has been studied as a means to induce stimulus response. Ultrasound can produce pressure waves with frequencies (20 kHz or higher) greater than that of human hearing. As well as audio and optical waves, ultrasonic waves can focus on a point, or reflect through a certain substance medium (such as water or air). Ultrasonic waves have enough penetrating ability and power to destroy a microcontainer shell and release the payload *in vivo*, deep inside the body [8]. In recent years, ultrasonic stimulation causing the drug release from multiple polymers has been used in biomedical fields. Ultrasonic stimulation can be applied as a remote control to a great number of polymers, such as multi-layered nanocapsules, micelles, polyelectrolyte nano-containers, liposomes that are sensitive to ultrasonic stimulation [9-16].

Ultrasound serves as a tool in disease diagnosis and therapy and has its unique advantages compared with other stimulations such as pH. pH-responsive polymers depend on the microenvironment in the body significantly. A slight change of pH value *in vivo* may affect the disease therapy. However, ultrasound treatment is not heavily dependent on its surroundings in the body. It has advantages of repetitive applicability, high safety profile, and cost-effectiveness [17]. The frequency of ultrasound should not be higher than human body tolerance. Otherwise, adjacent tissue and organs in the body may be injured. The ultrasonic stimulation (1MHz, 0.75-1.2 W/cm^2) used in this research would not cause harm to the human body. The use of multiple duty cycles (pulse/ pause, a percentage during one period in which the signal is active), especially at a relative high frequency, remains unexplored in drug delivery systems. Additionally, there remains a need to investigate the effects of ultrasonic stimulation inducing drug release from nanocapsules. In this study, polyelectrolyte nanocapsules containing the drug surrogate Rhodamine 6G as a drug delivery system were synthesised and the hypothesis that ultrasonic stimulation remotely induces dye release from the nanocapsules was investigated. Also, the

effect of addition of gold nanoparticles to the polyelectrolyte nanocapsules on the efficiency of ultrasonically induced dye release was determined.

1.2 Drug-eluting stents

Stent implantation surgery aims to keep arteries open for the treatment of coronary heart disease. Most patients with cardiovascular diseases undergoing surgery today are treated with stents. However, in-stent restenosis is a prominent problem affecting patients, with morbidity rates of between 10% and 60% reported. Restenosis is the term given to a section of blocked artery, previously opened up with the aid of a stent, that has become narrowed again [18-19]. Once the stents are placed in blood vessels, fresh tissue may grow inside stents, which will cover the struts of the stent. Initially, the fresh tissue consists of some healthy cells from the inner surface of the coronary artery. This is beneficial as a normal endothelial layer covering the stent allows for smooth blood flow. If this does not happen, scar tissue can form underneath the endothelial layer. Based on relative statistics, one quarter of patients who have a stent implanted had scar tissue formation [20]. This will produce a blockage and affect the blood circulation. Usually in-stent restenosis occurs between 3 to 6 months after stent implantation [21]. At present, drug-eluting stents (DES) have been employed as a treatment for in-stent restenosis. The efficacy and safety of DES rely on the kinetics of drug release, delivery system, and drug combination [22]. Two kinds of drug delivery stents have been studied, one with a polymer carrier and the other without a polymer carrier on the stent. In the case of anti-restenotic drugs loaded without a polymer, drug delivery was rapid and no significant benefits were observed [23]. However, when the drug was loaded with a polymer, the drug release has been proven to be more sustained and effective in reducing the risk of restenosis [24-25].

Some anti-restenotic drugs have been applied for DES previously. Sirolimus-eluting stents and paclitaxel-eluting stents have been shown to be effective in CAD treatment

[19, 26]. Sirolimus is a kind of macrocyclic lactone that binds to cytosolic proteins (FK506 binding protein). This binding protein blocks G1 to S cell cycle progression by preventing mTOR (mammalian target of rapamycin) activation [27]. Sirolimus also suppresses the proliferation of cytokine-driven T cells. Paclitaxel prevents the disassembly of microtubules and enables the polymerization of tubulin. This allows for the stabilization of the microtubules and leads to the prevention of cell division. The replication of the cell is prevented in the G_0/G_1 and G_2/M phases by paclitaxel [28]. In addition, paclitaxel affects cell transport and motility between organelles. Sirolimus and paclitaxel-eluting stents have been used with consistent results in treating in-stent restenosis [29].

1.3 Nanoparticulate carriers

The development of nanoparticle-based platforms provides an approach for disease diagnosis and therapy [30]. A nanoparticle is an ultrafine particle (typically around 100 nm or less in size) that works as a whole unit in terms of its properties or transport. Nanoparticles have a greater surface area per weight than larger particles, which cause them to be more reactive to some other molecules. Additionally, the optical property is one of the fundamental beneficial characteristics of a nanoparticle. Nanoparticles have been applied in wide variety of biomedical researches. Due to the side-effects of some bioactive substances used for pharmacotherapy, one of the goals in pharmacotherapy is to achieve specific drug delivery to an *in vivo* target site in a manner that minimizes side-effects and maximizes the therapeutic effect. For instance, cytotoxic compounds can kill cancer cells in cancer therapy, but also can injure normal cells causing undesired side-effects. Site-specific drug delivery with nanotechnology can make the drug encapsulated in carrier to reach the specific site and achieve drug release, which can minimize the side effects. Nanoparticulate delivery systems may also increase drug residence at specific sites and improve in

target-to-non-target concentration ratios. Furthermore, nanoparticles can be applied to nucleic acid-based therapeutic modalities to deliver the therapeutic molecules to sub-cellular compartments efficiently [31].

Nanocarriers can be synthesized from various materials including biodegradable and non-degradable polymers, metals, dendrimers, inorganic semiconductor nanocrystals and self-assembling amphiphilic molecules [30]. The selection of materials for the development of nanocarriers can be tailored to the desired therapeutic goals, the type of payload, the route of administration, and so on. The employment of stimuli-responsive nanocapsules provides an opportunity for drug delivery in specific sites. The selection of drugs is dependent on the therapeutic requirement, and drugs are usually adsorbed onto the nanocapsule cores. Additionally, the drugs encapsulated in nanocarriers could be injected into specific sites in the body. There is much literature dedicated to the research of nanoparticulate carrier systems based on the employment of lipid, polymeric, different types of nanoparticulate carriers, and self-assembling [30].

While the drug delivery system serves as an active vehicle in the treatment of diseases, the use of stimuli-responsive carriers provides an efficient method for drug release. Different kinds of molecular assemblies may be used as stimuli-responsive carriers for passive targeting and active targeting [32]. A nanocarrier with a desired stimuli-responsive property can be designed by a composition of these molecular assemblies. While the stimulus is distinct to the disease pathology, the stimuli-responsive carriers play an important role to respond specifically to the pathological “triggers”. Several biological stimuli such as redox, temperature and pH can be used for drug release in targeted sites [31, 33-36]. Usually, the intracellular or extracellular pH of the biosystem is significantly influenced by various diseases. For example, in solid tumors, the extracellular pH tends to be more acidic (~6.5) than the blood pH (~7.4) at body temperature [37]. Furthermore, the pH of lysosomal or

endosomal vesicles inside the cells is also lower than the cytosolic pH value. According to this characteristic, it is possible to fabricate nanocarriers that can respond changes in pH and allow for release of the encapsulated drug to targeted sites (extracellular or intracellular). In addition, a possible employment of films, such as 2-iminobiotin, for the controllable drug delivery is suggested. As demonstrated by Anzai's group, a kind of layer-by-layer assembly was achieved using avidin and 2-iminobiotin-labeled poly(ethyleneimine) (ib-PEI) [38-39]. The avidin binds 2-iminobiotin less strongly than biotin, and the affinity for 2-ininobiotin is pH dependent. Therefore the avidin-2-ininobiotin assembly can be disintegrated by either adding biotin in the solution or by changing the pH of the microenvironment (Figure 1) [38]. The findings also make it possible for further application of polyelectrolyte multilayer (PEM) carriers for the delivery of bioactive molecules in response to a known trigger [38-39].

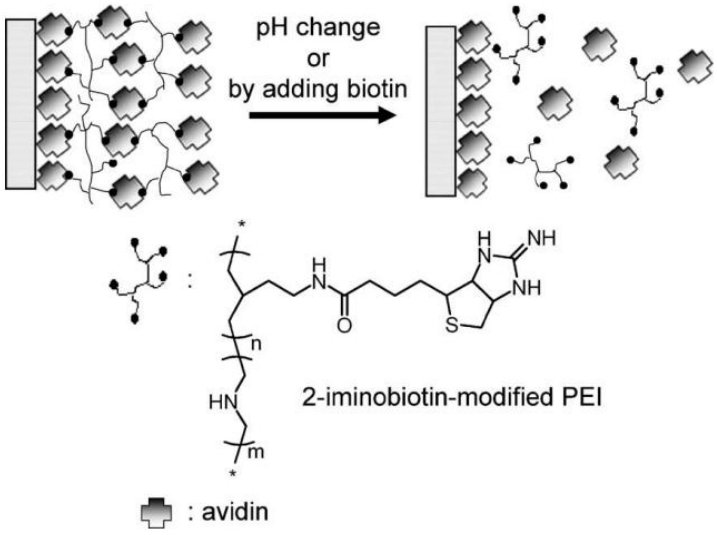

Figure 1 Decomposition of the avidin/2-iminobiotin-labeled poly(ethyleneimine) assembly stimulated by changes in pH or adding biotin [38].

Temperature is another variable which can be applied for inducing release of the

nanocarrier-payload drugs to a specific site [40]. For example, temperature-sensitive carriers could be employed to release the payload at temperatures above 37℃. By using this delivery system, the toxic drug would be completely encapsulated in the carrier and stable in the circulatory system. However, the drug would be easily available in a localised area, upon hyperthermic stimuli to the diseased region [40].

It is generally accepted that the redox potential in extracellular space or blood is low, but the redox potential inside the cells is high [41]. For example, the intracellular glutathione (GSH) levels in tumor cells are usually 100-1000 fold higher than extracellular levels [41]. By using disulphide cross-linked nanocarriers, this concentration gradient can be applied so that the encapsulated drug is delivered inside the cell. Such a system is significant in the release of nucleic acid-based therapies (like oligonucleotide, plasmid DNA), since these molecules have to reach intracellular targets in a steady manner to enable an efficient therapeutic effect.

External physical stimuli like heat, light, ultrasound and magnetic field can be employed to induce drug release from nanoparticulate carriers [42-46]. For example, the targeted delivery of iron oxide nanoparticles can be achieved by using a magnetic field. With the external stimulation, the materials encapsulated in the magnetic nanocarriers can accumulate at a desired site with a controllable manner [44]. In recent years, the efforts of many research groups have been focused on drug release from nanocarriers upon the application of ultrasound. For example, poly(ethylene glycol)-co-poly(h-benzyl-l-aspartate) micelles were used as drug nanocarriers, and the chemotherapeutic agent was encapsulated in the micelles [45-46]. A local ultrasonic stimulation was employed to achieve drug delivery in tumor cells after injecting the nanocarrier encapsulated drugs [45-46]. This method also achieves uniform distribution of the drug throughout the tumor tissue [47]. Additionally, light-responsive nanocapsules also have their distinct properties that achieve drug release upon external stimulation. Usually, the light-responsive nanocapsules are

sensitive to light sources. For example, upon the laser treatment, the gold nanoparticles within nanocapsules absorbs the laser light energy, and the heating caused from laser may destroy the capsules, resulting in drug release. Additionally, due to different components have different thermal expansion coefficients, the thermal stresses within the nanocapsule shell may also rupture the capsule shells, inducing the drug release [48]. Recent years have witnessed a growing interest in achieving active delivery of an encapsulated payload from polyelectrolyte multilayer nanocapsules by using near-infrared radiation (NIR) as a means of stimulation. In order to achieve nanocapsules with optical responsiveness, IR (Infrared radiation) dyes or gold nanoparticles were included in the polyelectrolyte multilayer carrier wall. The absorption of NIR induced heating and rupture of the carrier shells, and the release of polyelectrolyte multilayer carrier encapsulated drugs was achieved [49-50]. As reported, the responsiveness of nanocapsules can be achieved with a focused beam of CW laser at 830 nm [51], or with a short 8-10 ns laser pulses at 1034 nm (Figure 2) [49,50,52].

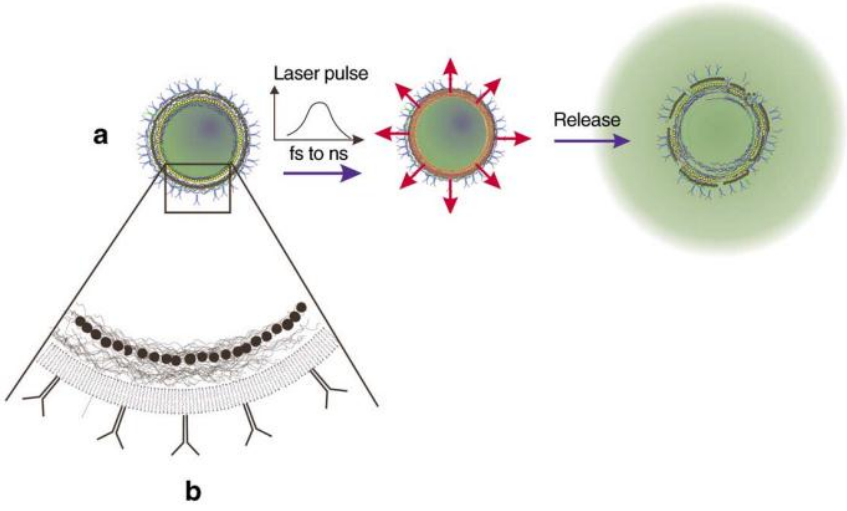

Figure 2 Schematic diagram of optical controllable nanocapsules. (a) the encapsulated material release triggered by irradiating the nanocapsules with a short laser pulse; (b) the cross-section of the shell of nanocapsule. (The shells contain gold nanoparticles, the outer lipid bilayer and the surface receptor molecules.) [52].

1.4 Ultrasound-responsive polymers

Many of the applications proposed for stimuli-responsive nanocapsules allow the controllable delivery of therapeutic compounds at the desired site within the body and at a specified release rate. In some conditions, by the migration of the nanocarrier encapsulated drug to a targeted site, the change in microenvironment necessary to impart responsive drug release can occur that encourages drug release. For example, pH-responsive nanocapsules can deliver drugs in the digestive tract due to the inherent differences in pH. Nonetheless, the application of a drug delivery system that depends on some other stimuli may be difficult by the inability to locally apply the stimulus at the desired areas. For example, a change in temperature may result in the drug delivery in the thermo-responsive nanocapsules *in vitro*, but localized heating and cooling *in vivo* is not always trivial at sites deep within the body.

However, ultrasound is an effective external stimulation that can induce the release of encapsulated drugs *in vivo* [53]. Ultrasound is the propagation of pressure waves through water or air, but at a frequency that is beyond the range of human hearing. Furthermore, ultrasonic waves can be absorbed, focused and reflected. Ultrasonic waves are the movement of molecules as the medium is expanded and compressed (at low pressure/at high pressure). Therefore, ultrasound can act upon biomolecules. In particular, ultrasonic waves are weakly absorbed by tissues and water, thus ultrasound can be employed to achieve effective energy transfer into the human body at targeted locations.

Ultrasound-responsive polymers for drug delivery system have been studied for medical diagnostics and treatment [54]. The mechanism of ultrasonic mediation applied in drug delivery system occurs in a process known as cavitation. Natural ultrasound energy can generate low and high pressure and causes the growth and shrinkage of gas-filled nanobubbles. Ultimately, the cavitating nanobubbles implode,

which can generate local shock waves and destroy polymer assemblies in the vicinity [55].

Some polymeric systems that respond to ultrasound are mainly polymeric micelles, gels or other layer-by-layer (LbL) coated nanoparticles. Langer et al., have studied the release rate of incorporated components through the stimulation of ultrasound from polymers including polylactides, biodegradable polyglycolides, and ethylene-vinyl acetate copolymers [56-62]. With an increase in ultrasound intensity, there was also an increase in the release dynamics in the polymeric systems. It has been shown that ultrasonic stimulation can facilitate the permeation through some polymers with no erosion and enhance the decomposition rate in some biodegradable polymers [63-64]. Miyazaki et al., studied the ethylene-vinyl alcohol (EVAL) copolymer and insulin in diabetic rats and were able to control insulin release through ultrasonic stimulation [65]. After the experimental subjects (diabetic rats) received the implants containing encapsulated insulin and experienced an ultrasonic stimulation (1 MHz, 1 W/cm^2), a significant decrease in the level of blood glucose was observed. The results demonstrated a rapid rate of release of insulin in the targeted region. In previous research of this group, they also demonstrated that the release rate of 5-fluorouracil from an EVAL copolymer increased at desired times upon the ultrasonic stimulation *in vivo* [66]. Stoodley et al., investigated antibiotic release from poly(2-hydroxyethyl methacrylate) (PHEMA) hydrogels by ultrasound irradiation (43 kHz) [56,67]. This drug delivery polymer matrix consists of a PHEMA hydrogel, coated with methylene chains to minimize passive drug release. The employment of low intensity ultrasonic stimulation may disrupt the alkane coating, and allow a significant drug release from PHEMA. In order to observe the performance of this drug delivery system for the targeting of infectious biofilms, the accumulation of pseudomonas aeruginosa biofilms grown on hydrogels was monitored, with and without exposure to ultrasonic stimulation in an *in vitro* flow cell study. Hung-Yin Lin et al., demonstrated the change in permeability of

poly(ethylene glycol) (PEG) encapsulated liposomes upon ultrasound (20 kHz, 3.8 W/cm^2) [68]. The results indicate that the rupture of liposomes in the sound field induced permeabilisation, and achieved the encapsulated material release. Additionally, the poly-and oligo(ethyleneoxide) additives seem to facilitate the rupture of liposomes. Ultrasound at relatively low frequency can facilitate the cellular uptake of the drug. Low frequency ultrasonic stimulation is also useful for drug delivery and can avoid damage to critical structures in the body. Pitt et al., have studied the hydrophobic drug (micelles were stabilized by copolymerizing with a biodegradable crosslinker N,N'-bis(acryloyl)cystamine) using low ultrasonic stimulation and have shown that the drug can be attached on PEO-b-PPO-b-PEO (poly(ethylene oxide)-block-poly(propylene oxide)-block-poly(ethylene oxide)) particles and achieved release with ultrasound. This means that the synergistic effects induced by ultrasound can cause efficacy enhancement, such as ultrasound-enhanced absorbance of drug into cells, and the ultrasound-responsive release of drug [69-73]. As illustrated by E. C. Pua et al., ultrasound treatment has been employed in gene therapy for therapeutic payload into the target cells [74]. Ultrasonic stimulation can induce the collapse of drug carriers and achieve payload release for the uptake of target cells (Figure 3). The site specificity can be promoted by incorporating a surface ligands on the carrier, which is able to bind to specific receptors for specific targeting.

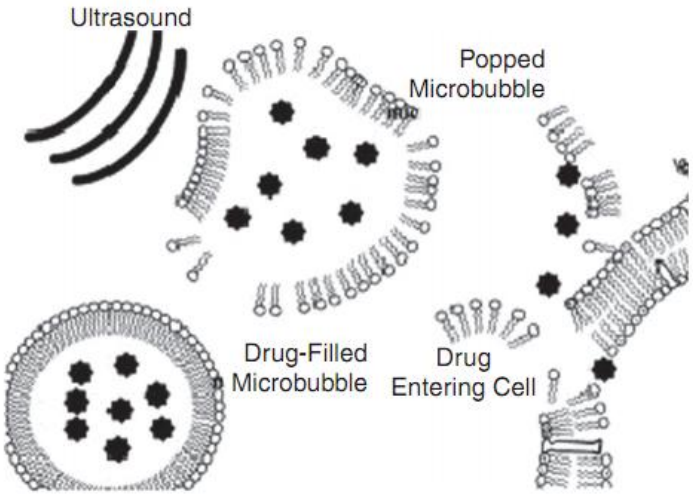

Figure 3 Schematic representation of encapsulated material release from polyelectrolyte capsules upon ultrasonic stimulation. DNA or therapeutic drugs can be incorporated into the interior of drug-and gas-filled micorbubbles. The drugs are released when ultrasound energy cavitates the microbubble [74].

Recent research has provided promising developments for administered drug carriers, where ultrasound is employed to induce changes in the carriers and release their payload. The employment of this type of drug/carrier combination can increase local drug delivery in a targeted site for improved efficacy.

1.5 Layer-by-layer technique for polyelectrolyte nanocapsule assembly

Polyelectrolyte nanocapsules are of further potential importance due to their extensive applications in medical fields. The capsule serves as a "medipack" to release a substance of interest at a specific site, and it has multiple outer layers to protect the core. Layer-by-layer techniques can be used for modifying surfaces and generating ordered functional polymeric films and nanocomposites over the substrate [75]. Such nanocomposites may include materials that are sensitive to different types of stimuli, hence resulting in an advanced delivery system with stimuli-responsiveness. In 1966, the layer-by-layer assembly was introduced by Iler

for the adsorption of multilayers of oppositely charged colloidal nanoparticles [76]. The assembly is based on the sequential adsorption of complementary multivalent molecules via non-electrostatic or electrostatic interactions. Additionally, the layer-by-layer assembly can be performed on different kinds of substrates of different shape, size and chemical composition (such as colloidal particles, porous and planar) using various building blocks, such as particles [77-91], dyes [92-94], polymers [95-110], clays [111-113], metal oxides [114-119]. Thus, using the layer-by-layer technique, polyelectrolyte nanocapsules with well-controlled size, shape, and flexible layer compositions can be obtained. Shell composition is predesigned and can contain lipid bilayers, biopolymers, magnetic nanoparticles and even charged polyions. The polyelectrolyte nanocapsule size is adjustable through the number of coating layers. Biodegradable polymer-based nanoparticles can be achieved by phase separation or by interfacial polymerization from a polymer-solvent mixture [120-122]. In previous research, lipid liposomes were employed as drug nanocarriers [123], which can be deposited on layer-by-layer polymer shells [124]. The method also indicates that there is no principle restriction to the option of polyelectrolyte.

The polyions commonly used include polycations, such as poly(allylamine hydrochloride) (PAH), poly(dimethyldiallyl ammonium chloride) (PDDA) and poly(ethyleneimine) (PEI), and polyanions such as poly(acrylic acid) (PAA), poly(vinyl sulfate) and Poly(styrene sulfonate) (PSS). The chemical structures of PAH and PSS are shown in Figure 4. For the successful assembly of protein multilayers, it is significant to employ linear polyion interlayers. Flexible linear polyions act as electrostatic glue in the layer-by-layer assemblies. The concept of electrostatic polyion glue, which keeps together neighboring arrays of proteins, is important to the protein and nanoparticle assembly. In our research group, layer-by-layer assemblies have also been used in the synthesis of multiple layers nanoparticles, which can be applied in drug delivery system for treatment of in-stent restenosis. Some findings and obstacles faced and possible solutions were studied.

The method to assemble microcapsules by nano-biotechnology was introduced by Noor Al-Nasser, and the microcapsules in aqueous solution was formed by Abraham Samuel Finny [125-126].

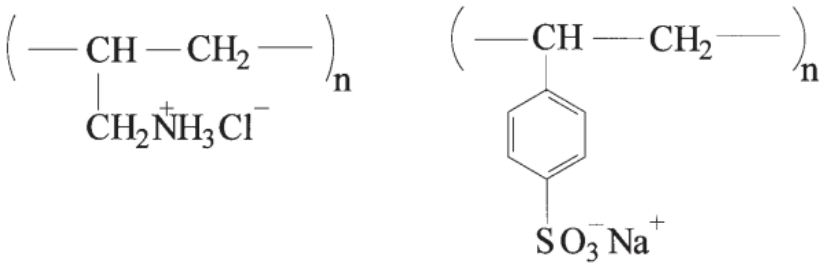

Poly(allylamine hydrochloride) (PAH+) Poly(styrene sulfonate) (PSS-)

Figure 4 Chemical structures of commonly used synthesis polymers.

The assembly procedure is shown in Figure 5 [127]. Firstly, a collection of nanotemplates or microtemplates, such as latex particle cores, with a negative charged surface are incubated in a solution including the cationic polyelectrolytes, and a layer of polycation is adsorbed. Secondly, the nanotemplates are washed by centrifugation, to remove the excess free polyions. The particles are then immersed in an anionic polyelectrolyte liquid. After one more layer is adsorbed, the original negative surface charge is restored and the surface is prepared for the next assembly. The two processes are alternately repeated to the point that the desired charge of outer layer of carriers or a layer of the desired thickness is achieved. Furthermore, more than two components can be employed in the layer-by-layer process but only with the correct alternation of negative and positive compounds.

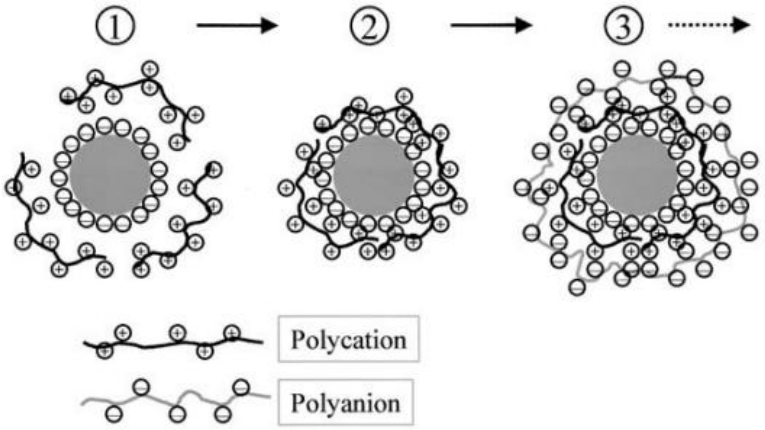

Figure 5 The layer-by-layer assembly on 3-Dnanotemplates [127].

In general, the layer-by-layer assembly shows obvious advantages: it achieves the integration of component materials of different properties within the films, and it makes the incorporation of various biomolecules into the films possible. Furthermore, it achieves a defined control over the thickness, structure, mechanical characteristics and composition of assembled materials [75].

1.6 Gold nanoparticles

Gold nanoparticles (AuNPs) have been studied for many years in applications such as cancer treatment [128]. They have high biocompatibility, ease of surface modification, facile synthesis, and tunable optical characteristics [129]. Colloidal gold is size controllable with a high yield, and high quality, which can be produced effectively using the method of citrate reduction [129]. In recent years, synthetic advancement engenders AuNPs of various structures or shapes, such as hollow gold nanoparticles, gold nanoshells, and gold nanorods. Their radiative properties are prominent, such as scattering, absorption and the plasmonic field, make these nanoparticles useful for molecular imaging [129]. Furthermore, metallic nanoparticles, such as gold nanoparticles, can support photothermal effects, the

dissipation of absorbed light energy as heat can be used to achieve drug release. As illustrated by Alexandra S. Angelatos et al., light-responsive nanocarriers have been achieved by incorporating metallic nanoparticles into the wall of the carrier [130-132]. With the application of short near-infrared laser pulses, the polyelectrolyte/gold nanoparticles nanocarriers rupture because of the gold nanoparticle-mediated heating of the carrier shell [130,131]. This idea was also proved to be workable for the release of fluorescence-labeled dextran [131]. Based on previous research, the release efficiency was investigated by coating gold nanoparticles in the microcapsules shell ($CaCO_3$ cores covered with 8-layered of polyelectyltes) [133]. Both the microcapsules with and without the gold nanoparticles in the shell were studied. With the application of ultrasound, the release efficiency was improved by the presence of gold nanoparticles in the microcapsule shell. The results also present a guide to incorporate a wide variety nanoparticles to tailor the properties of the microcapsules. In addition, gold nanoparticles are inert and are non-toxic, so they are a feasible material for medical applications [129,134,135].

Gold nanoparticles have distinct physicochemical properties such as surface plasmon resonance (SPR), and established surface modification chemistries allowing employment in a variety of biomedical applications [136]. In particular, after AuNPs were coated on the polyelectrolyte nanocapsules, the SPR may appear. The absorption mechanism of SPR is a collective coherent oscillation of the free electrons of the metal conduction band [137-140]. When a metal particle is exposed to light, a collective coherent oscillation of free electrons of the metal will be produced. The electron oscillation produces a charge separation relative to the ionic lattice, forming a dipole oscillation along the direction of the electric field of the light. At a specific frequency, the amplitude of the oscillation reaches maximum, and this phenomenon is called surface plasmon resonance. The nanoparticle is smaller than the incident light wavelength, and the response of a particle to the oscillating electric field can be

demonstrated by the dipole approximation of Mie theory [137,141]. In the approximation, the particle's extinction cross section is defined as $C_{ext}(\lambda)$ and it defines the energy losses in the propagation direction of the incident light resulting from the absorption and scattering of the nanoparticles. $C_{ext}(\lambda)$ can be demonstrated by the dielectric function of metal, $\varepsilon(\lambda)=\varepsilon'(\lambda)+i\varepsilon(\lambda)$. The dielectric constant of the medium is defined as ε_m, and it is shown in Equation 1 [141].

$$C_{ext}(\lambda)=\frac{24\pi^2R^3{\varepsilon_m}^{3/2}}{\lambda}\frac{\varepsilon''(\lambda)}{(\varepsilon'(\lambda)+2\varepsilon_m)+\varepsilon''(\lambda)^2} \quad (1)$$

Where R is the radius of particle, and λ is the incident light wavelength.

As shown in Equation 1, the extinction cross-section of a single nanoparticle relies on the dielectric function of the metal of which the particle is composed. This leads to different scattering and absorption features for different metal particles. Furthermore, the maximum of $C_{ext}(\lambda)$ will occurred when the denominator of the right side of the equation is minimised. This happens at the wavelength λ_p for which $\varepsilon'(\lambda_p)=-2\varepsilon_m$, when the imaginary part of the metal dielectric function, $\varepsilon'(\lambda_p)$, is small [137,141].

1.7 Experimental objectives

The work in this research is to develop a smart nanostructured drug delivery system, controlled using ultrasonic stimulation. Published studies showed that nanocapsules loaded with drugs have been used as tools in therapeutic fields, which is a potential

clinical application. This research focused on polyelectrolytes polylactic acid (PLA), poly(allylamine hydrochloride) (PAH), and poly(styrene sulfonate) (PSS) for their feasibility and function as drug carriers. Various ultrasound duty cycles (low, medium, and high, 0.75-1.2 W/cm^2) at a frequency of 1 MHz were used as a remote stimulation on nanocapsules for drug release. The duty cycle is defined as the percentage during one period in which the signal is active [128]. The ultrasonic frequency used in this study is safe to the human body. Rhodamine 6G, a kind of fluorescein dye, encapsulated in nanocapsules was used as a drug surrogate in this model system for controlled release studies. The experimental procedures for forming the multi-layer nanocapsules and the ultrasonic stimulation process is described in Figure 6.

The core of the nanocapsule is made up of PLA nanoparticles. The Rhodamine 6G dye serves as a tracer material in place of anti-restenotic drugs. It can be easily detected by photophysical measurements. The layers coated on PLA cores contain PAH polymers (positively charged), PSS polymer (negatively charged) and gold nanoparticles (negatively charged). With the opposite charge on polyelectrolytes, the nanocapsules can be formed and the number of layers can be varied as required. In each layer, the absorbance measurement aims to detect the variation in layer-by-layer assemblies. Zeta potential measurements were also adopted to check the layer processing. In terms of remote ultrasonic stimulation process, the nanocapsules suspended in liquid can be stimulated. In the further clinical application, the system aims to allow the drug release from drug-eluting stent in a controllable manner. Ultrasonic stimulation can be employed to trigger drug release from nanocapsules. Anti-restenotic drug released under controlled conditions with ultrasonic stimulation can be used to inhibit smooth muscle cells proliferation and heal arterial walls. Experimental results and discussion of drug delivery systems working with different duty cycles of ultrasonic stimulation will be combined so as to illustrate the implications of these results.

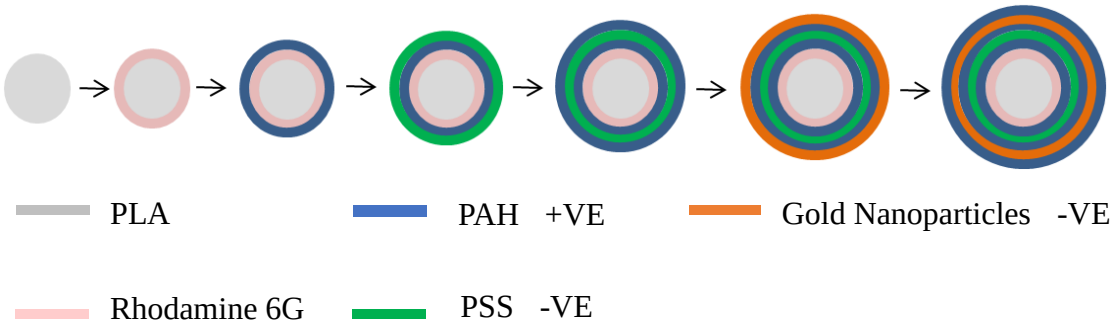

Figure 6 The layering processes of nanocapsules. The grey sphere represents the PLA nano-cores; the pink layer represents the Rh6G which serves as a tracer material in place of anti-restenotic drugs; the blue layer represents the PAH layer which is positively charged; the green layer represents the PSS layer which is negatively charged; the gold layer represents the gold nanoparticles which is negatively charged.

Chapter 2: Materials and methods

2.1 Materials

Poly (D,L-lactide) (M_w=10,000~18,000), Poly (allylamine hydrochloride) (M_w= ~58,000), Poly(styrene sulfonate) (M_w= ~70,000), Rhodamine 6G (M_w=479.01), Acetone (M_w=58.08), Gold(III) chloride trihydrate (M_w=393.83), Sodium citrate dehydrate (M_w=294.10), Sodium chloride (M_w=58.08) were obtained from Sigma Aldrich and used without further purification. The presence of 6 mM of NaCl in PAH and PSS solution enabled the anticoagulant function of polymers.

2.2 Synthesis of polylactic acid (PLA) nanocapsules

2.2.1 PLA nanocapsule core

PLA is a kind of polymer with biocompatible and biodegradable properties. The chemical structure of PLA is shown in Figure 7. PLA can be broken down to the monomeric units of lactic acid, and the lactic acid can be converted into glucose by the liver, and then the glucose is employed as energy in the body. Therefore, PLA nanocapsules are devoid of any major toxicity.

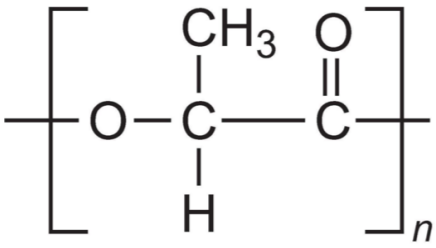

Figure 7 The chemical structure of PLA.

PLA nanocapsules were produced by using a nanoprecipitation method, and the

method has been introduced in previous research [142]. The main procedure to generate PLA/Rhodamine 6G nanocapsules is as follows: 20 mg of PLA was dissolved in 5 mL of acetone and equilibrated for 12 hours at room temperature. Next, 0.1 mg of Rhodamine 6G was added to the acetone solution. Gradually, the colour changes of acetone solution were observed from colourless to bright red due to Rhodamine 6G becoming dissolved. The organic solution was stirred at 800 rpm for 2 hours using a stirrer hotplate, which allows the PLA and Rhodamine 6G to completely attach. Rhodamine 6G is a substance sensitive to light, so the stirring process should be carried out in a dark environment. After stirring, the organic solution was added drop by drop within 2 minutes into 50 mL of distilled water containing no surfactant, under appropriate stirring (1000 rpm) for 2 hours. After injecting the organic phase to the aqueous phase, a conspecific nanodispersion can be obtained. Acetone in the solution was removed from the dispersion by evaporation in chemical hood. The PLA nanocapsules were suspended in 25 mL of water through centrifugation (6000 rpm) for 20 minutes. The resuspended PLA nanocapsules were pipetted 1 mL for Ultraviolet-visible (UV-vis) measurement, which allows the changes during layer-by-layer assemblies to be measured. The PLA/Rhodamine 6G capsules served as cores of the nanocapsules for the next layer-by-layer assemblies.

2.2.2 Synthesis of gold nanoparticles

Gold is a metallic element with a boiling point of 2800 ℃, and a melting point of 1064 ℃. The $HAuCl_4$ chemical structure is shown in Figure 8. Due to some properties of gold, such as conductivity, biocompatibility and its inability to react with oxygen and water, it has been used in biomedical fields over time [143-145].

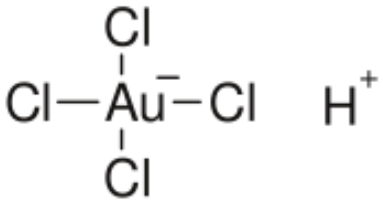

Figure 8 The HAuCl4 chemical structure.

The gold nanoparticles were generated by following the method previously published by *Bastus* in 2011 [146]. In brief, a solution of 2.2 mM sodium citrate in distilled water (150 mL) was heated with hotplate in a 250 mL beaker for 15 min under stirring (1100 rpm/min). When the solution is boiled, 1 mL of $HAuCl_4$ (25 mM) was added. Then the beaker was removed from hotplate, and left to cool down. The solution color changed from yellow to bluish gray and then to deep red in 15 minutes. The prominent variety of the solution color reveals that the gold nanoparticles were successfully synthesized. The resulting particles were coated with citrate ions (negatively charged) and are then suspended in distilled water. The size of the gold nanoparticles was ~13 nm, and the concentration was ~3 x 10^{12} NPs/mL [146]. In order to check the resulting gold nanoparticles, UV-visible measurement was conducted on a Jasco UV-visible spectrophotometer, from 450 nm to 650 nm.

2.2.3 Layer-by-layer assemblies

PLA nanocapsules consists of PLA core, PAH, PSS and gold nanoparticles shells fabricated by layer-by-layer assembly technique. In brief, 37.5 mL of PAH (1 mg/mL, positively charged) aqueous solution was added to 25 mL of the PLA cores and the mixture was stirred for 2 hours at a speed of 800 rpm, to make interaction between the PLA capsules and PAH solution. The solution was centrifuged for 15 minutes at 13000 rpm, and the supernatant was removed. The PAH coated nanocapsules were

resuspended in 31 mL of distilled water for the next layer assemble. For the second polyelectrolyte layer coating, 46.5 mL of PSS (1 mg/mL, negatively charged) was added into 31 mL of the PAH coated capsules and the hybrid was stirred for 2 hours again at a speed of 800 rpm. After centrifuging employing the same parameters, PAH/PSS coated nanocapsules were re-suspended in 38 mL of distilled water. Similarly, PAH was employed to form the third layer. Following the same assembly technique mentioned, PAH (positively charged) coatings were achieved. The PAH/PSS/PAH coated nanocapsules were again dispersed in 47 mL of water. Once the PLA capsules undergo three successive layers, 28.2 mL of negatively charged gold nanoparticles aqueous (25 mM) which was previously prepared was added. The mixture solution was vigorously stirred for 2 hours, and the resulting suspension was transferred to a beaker for the last PAH layer coating. PLA/Rhodamine 6G/PAH/PSS/AuNPs/PAH core-shell structure composite nanocapsules were obtained after centrifugal separation of re-suspension, and then prepared for the ultrasonic stimulation experiments.

2.3 PLA nanocapsule characterization

Scanning electron microscope (SEM) analysis of the PLA nanocapsules was carried out on a TM-1000 electron microscope (Japan Hitachi Co.) operated at an accelerating voltage of 15 kV. Measurement of charge distribution on nanocapsules surface was performed by using zeta-potential (Britain Malvern Co.) at room temperature. Photophysical characterization of the nanocapsules was conducted by a UV-visible spectrophotometer (Japan Jasco Co.) at room temperature. Fluorescent measurements of Rhodamine 6G were conducted on a FluoroLog fluorimeter (Japan Horiba Co.) at room temperature.

2.3.1 Determination of PLA nanocapsule morphology by SEM

SEM is widely applied in industry and academia for the study of composition and surface topography. A high energy electron beam was employed to make various signals at the solid specimens surface. The signals provide information about the sample such as crystalline structure and external morphology. Usually, the data is collected over a selected area of the sample surface, and an image is achieved that shows spatial variations in the properties. The magnification range of the SEM used is from 60x to approximately 10,000x, and spatial resolution of down to 35 nm, which is much better than a normal optical microscope. The working principle of SEM is shown in Figure 9 [147].

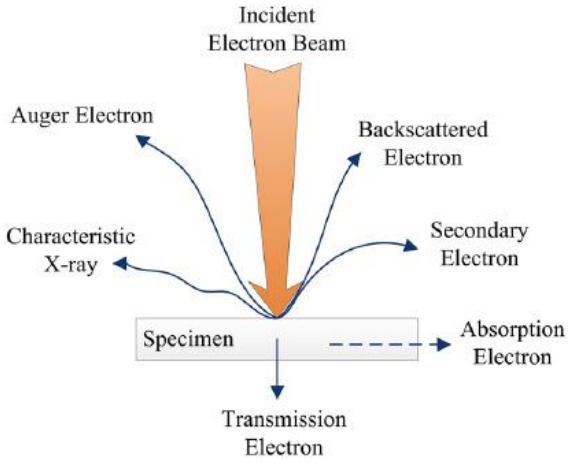

Figure 9 The SEM working principle [147].

In SEM, electrons are accelerated via an electric field and are focused onto the surface, hitting the sample with a certain kinetic energy. While the incident electrons are decelerated in a sample, the kinetic energy is dissipated as various signals. The signals contain backscattered electrons, secondary electrons (that generate SEM images), auger electrons (that are used for surface sensitive composition information) and characteristic X-rays. The electron beam impinges onto the sample and the

signals introduced will be emitted from the impinged position. The signals on the substance surface are detected and the signal intensity is amplified at the same time, which serves as the intensity of the pixel on an image displayed on the laptop screen. Different positions of the sample will be bombarded by the intensive electron beam one by one and the detected intensity gives the intensity in the next pixel and by this analogy.

Sample preparation is important for SEM analysis. In particular, the preparation should make sure the sample will fit into the chamber to inhibit charge build-up on electrically insulating sample. Most electrically insulating samples are sprayed with conducting material, such as gold or carbon.

In this research, the sample surface was deposited with conductive gold for better surface detection. A drop of nanocapsules sample was pipetted out to spread on a piece of glass slide and dried in the chemical hood.

2.3.2 Photophysical measurements of PLA nanocapsules

UV-vis spectroscopy is employed to acquire the absorbance spectrum of a sample in liquid. In principle, the absorbance of electromagnetic radiation or light energy allows the electrons transfer to the excited state from the ground state of the compound. The Beer-Lambert Law, a principle behind the absorbance spectroscopy is critical, and the formula is shown in Equation 2.

$$A = \log I_0 / I = \varepsilon bc \tag{2}$$

For a single wavelength, A is the absorbance, ε is the molar absorptivity of the

compound in liquid ($M^{-1}cm^{-1}$), b is the path length of a cuvette (usually 1 cm), and c is the liquid concentration (M). A light beam derived from UV light is separated into its component wavelengths by a prism. Every monochromatic beam is separated into two equal intensity beams in turn by a half mirror. One beam passes through the compound solution cuvette, and the other beam passes through the reference solvent. The solvents should be completely transparent and the most commonly employed solvents are ethanol, water, cyclohexane or hexane. The intensities of the light beams will be measured by electronic detectors and compared.

The intensity of sample beam is defined as I, and the intensity of reference beam is I_0. In a short time, the spectrometer scans the component wavelengths automatically. If the sample absorbs the light at a given wavelength, $I < I_0$. When the sample cannot absorb the light, $I = I_0$. Absorption is presented as absorbance (A), and the wavelength of maximum absorbance (λ_{max}) depends on different compounds.

In a UV-vis spectroscopy measurement, the transmittance of the sample (T) is defined as the fraction of photons (I) that pass through the sample over the incident photons (I_0). For example, at $T = I/I_0$, the photons measured are not scattered and absorbed by a sample. Usually, the absorbance (A) of a sample is reported, which is related to the transmittance by $A = -\log_{10}(T)$.

The UV-vis spectroscopic measurement can provide qualitative or quantitative information of a molecule or compound. Referencing of the instrument is required before analysis can be undertaken, this comprises of using a reference cuvette of the solvent being used. This is crucial whether qualitative or quantitative analysis is desired. For quantitative measurement of the compound, it is necessary to calibrate the instrument. Therefore, known concentrations of the compound of interest in a solution are required and the same solvent has to be used for the unknown sample.

Fluorescence was first observed by Monardes in 1565 [148]. Fluorescence may be described through a Jablonski diagram, shown in Figure 10 [148-149]. This demonstrates the electron transfer between the electronic states of a molecule. Before light of wavelength k_{ex} impacts on a molecule, the electron occupies the ground state. The incoming light should have an energy equivalent to or larger than the band gap to facilitate transfer of an electron into a vibrational energy state (S_2). An excited state electron loses its energy rapidly (approximately 10^{-12} seconds), a process called internal conversion, and transfers to the lowest vibrational energy level (S_1). During the next transition, the electron falls back into the ground state (S_0) by spontaneous emission or non-radiative decay. In the first case energy is released in the form of a photon, in the second case by releasing energy in the form of heat. Additionally, when a non-radiative vibrational transition appears between a singlet ground state (S_1) and an excited triple state (T_1), phosphorescence will happen. Phosphorescence transition is not difficult to distinguish from the fluorescence, since that phosphorescence transition occurs much more slowly than fluorescence (time scale is from minutes to hours).

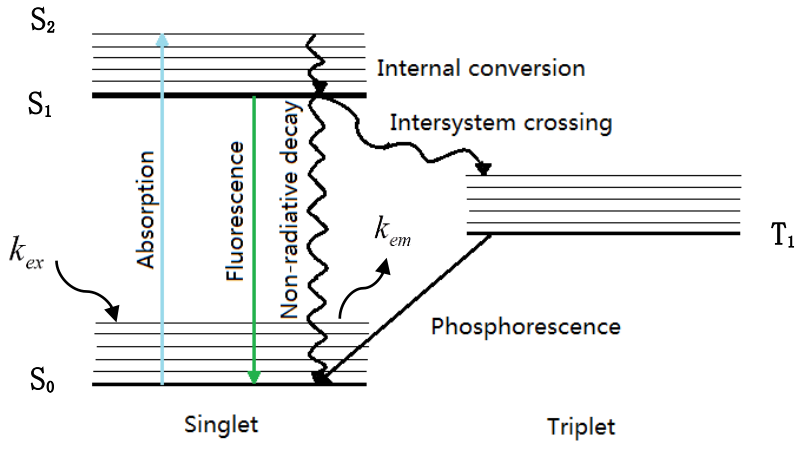

Figure 10 Jablonski diagram showing the radiative photophysical processes (absorption, fluorescence, and phosphorescence) and non-radiative photophysical processes (internal conversion and intersystem crossing) [149].

During the synthesis of PLA/Rhodamine 6G capsules and each layering stage with PAH, PSS or gold nanoparticles, the nanocapsules solution and the supernatant of final samples were analyzed using UV-visible Spectrophotometer, FluoroLog machine and zeta potential measurement to confirm the uptake of Rhodamine 6G dye by the PLA nanocapsules and layer-by-layer assemblies.

Rhodamine 6G is a fluorescent Rhodamine dye, and its fluorescence is intense. The Rhodamine 6G chemical structure is shown in Figure 11.

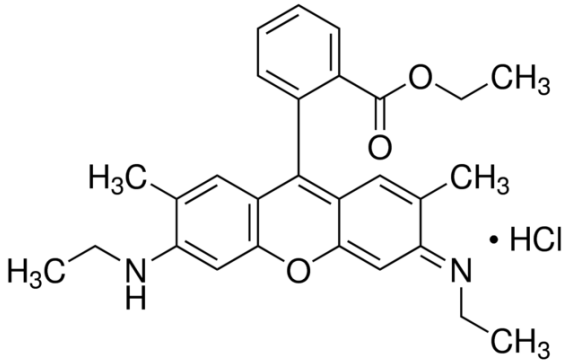

Figure 11 Rhodamine 6G chemical structure.

Normally, Rhodamine is extracted from xanthene and serves as tracer agent or active medium in photophysical analyses. Due to the fact that it is highly fluorescent, Rhodamine 6G is served as a probe instead of a drug in this research, and its excitation wavelength is about 526 nm. In order to obtain the PLA capsules containing Rhodamine 6G, 4 mL of PLA/acetone solution was mixed with 0.1 mg of Rhodamine 6G (5.22×10^{-5} mol/L) under stirring for 2 hours before synthesis of PLA/Rhodamine 6G capsules. With photophysical machines (both UV-vis and FluoroLog), Rhodamine 6G existed in capsules or supernatant and can be detected during the synthesis of PLA/Rhodamine 6G/PAH/PSS/AuNPs/PAH capsules and dye release under ultrasonic stimulation [150-153].

Fluorescence intensity was detected using a FluorLog machine. Compared with absorption and fluorescence emission spectra, specific optical characteristics can be observed and conclusions drawn. Since the excitation peak (λ_{max}) of Rhodamine 6G is approximately 526 nm, the wavelength range was set between 300-700 nm for absorption spectra analyses and 530-700 nm for fluorescence emission spectra measurements. The excitation wavelength of gold nanoparticles is about 519 nm, which may be overlap with that of Rhodamine 6G, thus whether the dye released or not was detected by the fluorescence emission spectra measured. Before and after ultrasonic stimulation, the PLA/Rhodamine 6G/PAH/PSS/PAH/AuNPs/PAH nanocapsules were suspended in distilled water and the supernatant was measured by FluorLog machine. Whether dye release is working or not can be observed by the fluorescence intensity change in the emission spectra taken from supernatants of nanocapsules solution (The supernatant was collected from the nanocapsules solution by centrifugation after each ultrasonic stimulation). The data obtained was produced as curves or graphs for further analyses.

2.4 Ultrasonic stimulation

Ultralieve is a hand-held ultrasound device employed for the stimulation of the PLA/Rhodamine 6G/PAH/PSS/PAH/AuNPs/PAH nanocapsules in this research. The technology of therapeutic ultrasound is a high frequency sound vibration which cannot be felt by humans, and can stimulate tissue up to 5 cm beneath the skin's surface. The ultrasonic frequency is 1 MHz and the duty cycle contains three different levels including Low (30% duty cycle, 0.75 W/cm^2), Medium (40% duty cycle, 1.0 W/cm^2) and High (50% duty cycle, 1.2 W/cm^2). After synthesizing the nanocapsules, they were suspended in distilled water and were stimulated by the *Ultralieve* device at different duty cycles (low, medium, and high), and then the supernatant was used for fluorescence emission spectral analysis and comparison.

The schematic diagram of ultrasonic stimulation imparts onto the nanocapsules is shown in Figure 12.

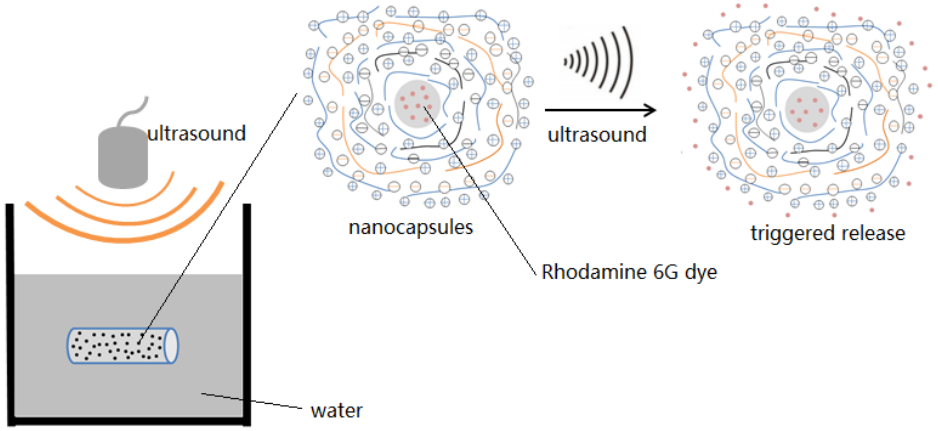

Figure 12 Schematic diagram of ultrasonic stimulation imparts onto the nanocapsules. The PLA/Rh6G/PAH/PSS/PAH/AuNPs/PAH nanocapsules were suspended in the tube and the tube was fixed in water. The ultrasound device was fixed and kept working, which is shown on the left of Figure 12. In the nanocapsules details showed on the right of Figure 12, the gray spheres represent the PLA nanocapsules, the red particles represent Rh6G dye, the blue curves represent PAH layer (positively charged), the black curves represent PSS layer (negatively charged), and the yellow curves represent AuNPs shell. The dye may be released by the stimulation of ultrasound.

The duty cycle is defined as percentage during one period in which the signal is active [154]. The period represents the time of a signal completing one on-and-off cycle. The duty cycle can be shown as an equation:

$$D = \frac{T}{P} \times 100\% \tag{3}$$

In Equation 3, D represents duty cycle, $T(\mu s)$ represents the duration of active

signal, and $P(\mu s)$ represents total duration of signal. For example, a 30% duty cycle pulsed waveform would have ultrasound on for a total of 30% of the entire treatment, and off for a total of 70%. A 100% duty cycle is the same as "continuous". For the device used in this research, the duty cycle is fixed which includes 30%, 40% and 50%.

Ultrasound waves propagate in fluids and solids. The mechanical perturbation produces disturbances of the medium particles, and these disturbances provoke a displacement of the particles and are transmitted to other parts of the medium. In particular, the ultrasound wave propagation relies on the intrinsic elastic properties of the medium. Fluids support bulk compression waves (longitudinal waves), which are characterized by the medium density changes. The particles in this medium oscillate in the longitudinal direction. Additionally, bulk compression waves can propagate in solids. Biological tissues are viscielastic solids. Both longitudinal and shear waves can propagate in tissues. However, in soft tissues, ultrasound shear waves are usually neglected since shear waves are highly attenuated at ultrasonic frequencies [155]. One of the typical propagation properties of ultrasound propagation in materials is speed. The speed at which ultrasound waves propagate in a fluid can be described in Equation 4 (assumed to be an adiabatic process) [156-158].

$$V = \sqrt{\frac{E}{\rho}} \tag{4}$$

Where E is a factor related to the elastic properties or "stiffness" of the material, and ρ is the density of the material.

In an isotropic solid, both longitudinal and shear waves are supported in which their respective propagation speeds are given in Equation 5 and Equation 6 [156-158].

$$C_L = \sqrt{\frac{\gamma(1-\sigma)}{\rho(1+\sigma)(1-2\sigma)}} \tag{5}$$

$$C_S = \sqrt{\frac{\gamma}{2\rho(1+\sigma)}} \tag{6}$$

Where γ is the Young's modulus and σ is the Poisson ratio. Since σ is less than 0.5, C_L is greater than C_s.

The speed of ultrasound wave propagation is dependent on the density and elastic properties of the materials. The propagation speed of sound in bones is greater than that in soft tissue and water [155]. Additionally, the propagation length may also affect the propagation efficiency of ultrasound waves.

Chapter 3: Results and discussion

The synthesis of PLA/Rhodamine 6G/PAH/PSS/PAH/AuNPs/PAH nanocapsules was achieved by a layer-by-layer technique. Rhodamine 6G dye, in place of anti-restenotic drugs, was adsorbed onto PLA nanocapsules in this research. After each ultrasonic stimulation on nanocapsules, the release of dye was observed using fluorescence spectroscopy. The data were collected and analyzed and the results are presented below.

3.1 SEM analysis of PLA/Rhodamine 6G/PAH/PSS/PAH/AuNPs/PAH nanocapsules

PLA/Rhodamine 6G/PAH/PSS/PAH/AuNPs/PAH nanocapsules were prepared by alternate deposition of cationic polymers (PAH) and anionic polymers (PSS) onto PLA cores. PLA/Rhodamine 6G/PAH/PSS/PAH/AuNPs/PAH nanocapsules were suspended in distilled water and one drop was placed onto a cover slip. After drying for 24 hours, the sample was analysed by SEM. A SEM image of the nanocapsules is shown in Figure 13.

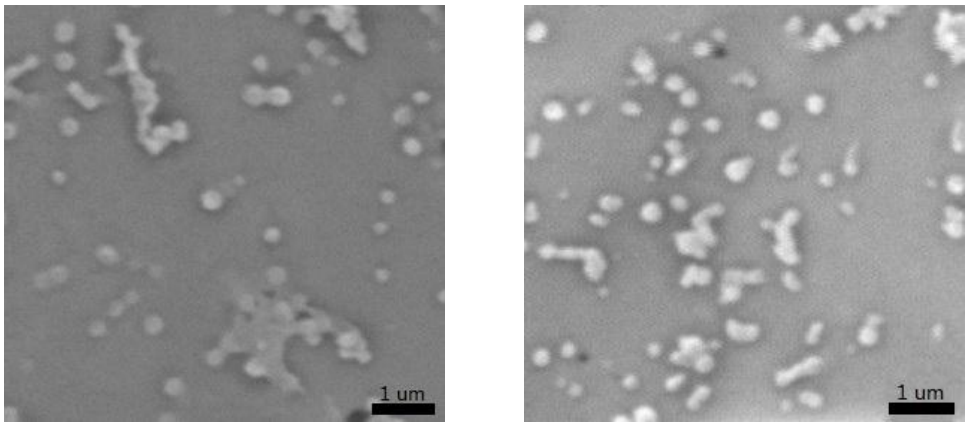

(a) (b)

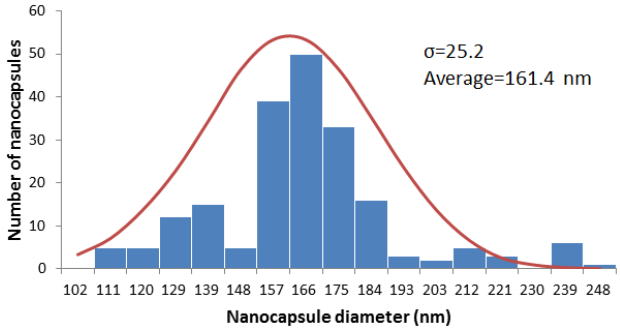

(c)

Figure13 (a) and (b) SEM image of PLA/Rh6G/PAH/PSS/PAH/AuNPs/PAH nanocapsules. (c) The size distribution of nanocapsules. The samples for size measurement was collected from 200 nanocapsules.

Figure 13 shows that the typical PLA/Rhodamine 6G/PAH/PSS/PAH/AuNPs/PAH nanocapsules have spherical shapes, with a size 165±25.2 nm. The size of nanocapsules was measured by using software named ImageJ. ImageJ is a Java-based image processing program, and it can be used for diameter measurement. For diameter, the straight line across the center of the nanocapsules was drawn to find out the exact value for the "length".

3.2 Absorbance and fluorescence emission spectra of pure Rhodamine 6G dye

Rhodamine 6G dye has specific optical characteristics [159-160]. The dye has a high photostability, high fluorescence quantum yield, and its lasing range is close to its absorption maximum (around 530 nm) [161]. The absorption and fluorescence emission spectra are unique. The absorption and fluorescence spectra of pure Rhodamine 6G in water are shown in Figure 14.

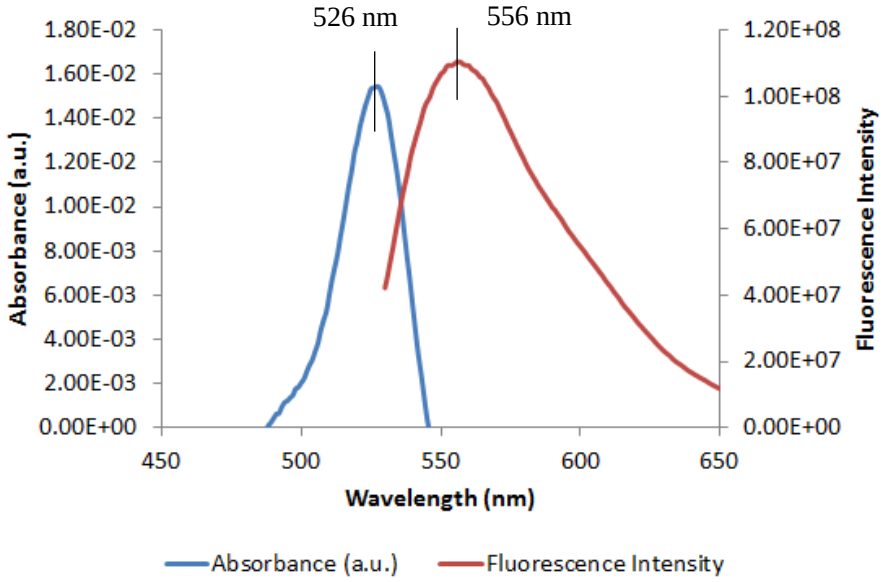

Figure 14 The UV-vis absorption and fluorescence emission spectra of pure Rh6G in water.

The UV-vis absorption spectrum of pure Rhodamine 6G (dissolved in water, 1 mL) has a peak at λ_{abs}~ 526 nm. The concentration of pure Rhodamine 6G, shown in Figure 14, is 2.09 x 10^{-7} mol/L. The concentration is based on Beer-Lambert law. The fluorescence spectra recorded for Rhodamine 6G in water, excited at λ_{abs}=526 nm, revealed an emission peak at 556 nm.

A cuvette of colloidal gold nanoparticles (1 mL) was collected for UV-vis measurement. The result is shown in Figure 15.

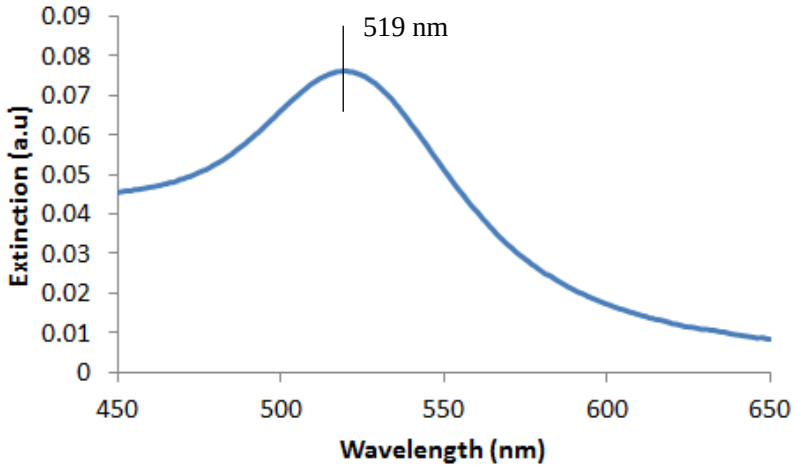

Figure 15 UV-vis extinction spectrum of colloidal gold nanoparticles.

The UV-vis extinction spectrum of colloidal gold nanoparticles has a peak at λ_{ex} ~ 519 nm. The concentration of gold nanoparticles, shown in Figure 15, is 3.15 x 10^{-9} mol/L (particle size is 13 nm, extinction coefficient (ε_{max}) is 2.42x 10^{8} [162]).

The absorbance peak of Rhodamine 6G (λ_{ex} =526 nm) is overlapped with that of gold nanoparticles (λ_{ex} =519 nm). Therefore fluorescence intensity of Rhodamine 6G is used in this study to indicate the concentration of Rhodamine 6G. To this end, the correlation between the fluorescence intensity of Rhodamine 6G with the concentration of Rhodamine 6G was quantified. The linear relation between Rhodamine 6G concentration and fluorescence emission intensity is shown in Figure 16. Thus, the changes of dye released from nanocapsules upon ultrasonic stimulation were monitored by the changes of fluorescence intensity of Rhodamine 6G in solution.

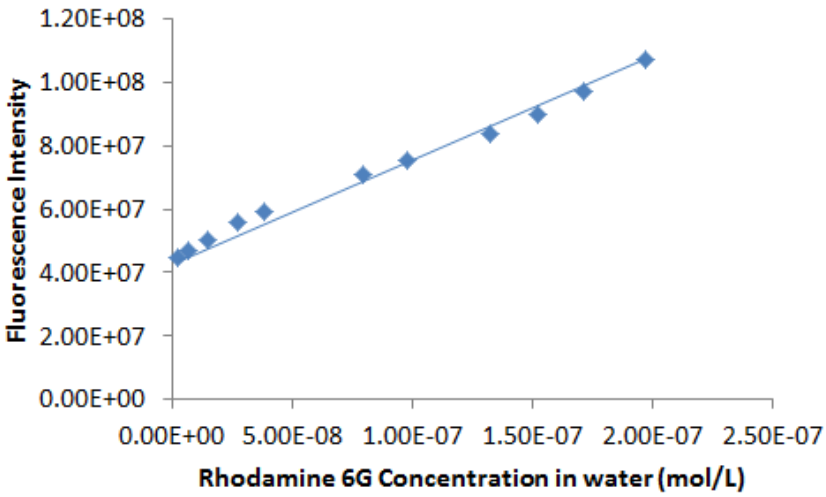

Figure 16 The relationship of Rh6G concentration and fluorescence intensity in water.

3.3 Characterisation of nanocapsule assemblies

In this research, the nanocapsules were synthesized with four polymer layers and one AuNPs layer, which contain opposite charges, via a layer-by-layer self-assembly process. After the formation of PLA capsules containing Rhodamine 6G, the nanocapsule solution (1 mL) was collected for UV-vis measurement, to confirm the presence of Rhodamine 6G. The absorbance spectrum of PLA/Rhodamine 6G nanocapsules is shown in Figure 17.

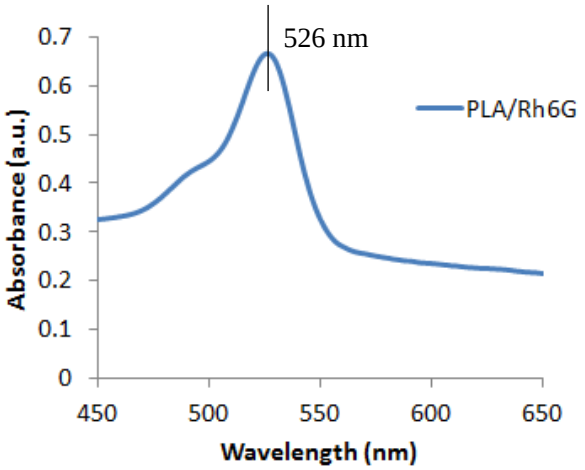

Figure 17 UV-vis absorbance spectrum of PLA/Rh6G nanocapsules.

Figure 17 shows an absorption peak at 526 nm, indicative of the typical Rhodamine 6G absorption. This indicates that Rhodamine 6G has been successfully included in the PLA capsules.

To examine the layer-by-layer assemblies of PAH, PSS and AuNPs on the dye functionalised PLA nanocapsules, the sequential adsorption procedures were monitored by means of zeta potential. The variation of zeta potential with the sequential adsorption of polyelectrolyte layer for PAH/PSS/PAH/AuNPs/PAH coatings is shown in Figure 18.

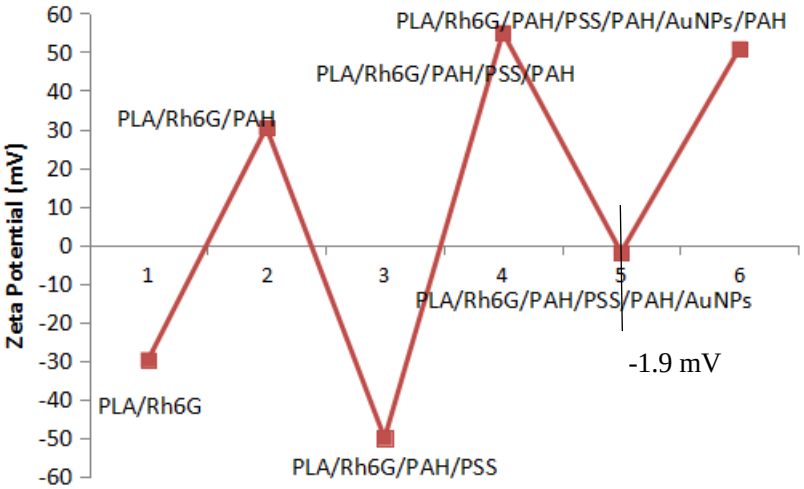

Figure 18 Zeta potential measurements in the layer-by-layer assemblies of nanocapsules.

The zeta potential value of pristine PLA nanocapsules was negative (-34.5 mV). This may be due to the carboxylic groups present on the surface of the PLA nanocapsules [163]. Therefore, the adsorption of cationic polymers (PAH) on the PLA/Rhodamine 6G nanocapsules (negatively charged) was possible. It was observed from the zeta potential measurements that the adsorption of a positively charged PAH layer on PLA/Rhodamine 6G nanocapsules changes the zeta potential from -34.5 mV to +30.4 mV. Subsequently, deposition of a negatively charged PSS layer leads to another

potential reversal from +30.4 to -50 mV. Further alternating the deposition of the PAH, AuNPs and PAH led to continuous reversals in zeta potentials. This reveals a stepwise layer assembly during the fabrication of composite nanocapsules. It is clear that the gold nanoparticles (negatively charged) adsorbed onto the PAH layer (positively charged) at a good surface coverage which screened the underlying positive charge but does not create a highly charged negative surface, unlike when other polymer layer by layer coatings are performed. The zeta potential value of nanocapsules after coating gold nanoparticles is -1.9 mV. A low negative zeta-potential means that the colloid will not be very stable compared to a larger positive or negative potential values. This requires further study to confirm the reasons and make improvements. Therefore, it seems that another polymer layer is necessary after gold nanoparticles coating for maintaining the stability of the capsules.

After coating AuNPs onto the PLA/Rhodamine 6G/PAH/PSS/PAH nanocapsules, the nanocapsule sample (1 mL) was collected for UV-vis measurement. The result is shown in Figure 19 (a). Additionally, the UV-vis measurement for PLA/Rhodamine 6G/PAH/PSS/PAH was also carried out as a comparison, and the result is shown in Figure 19 (b).

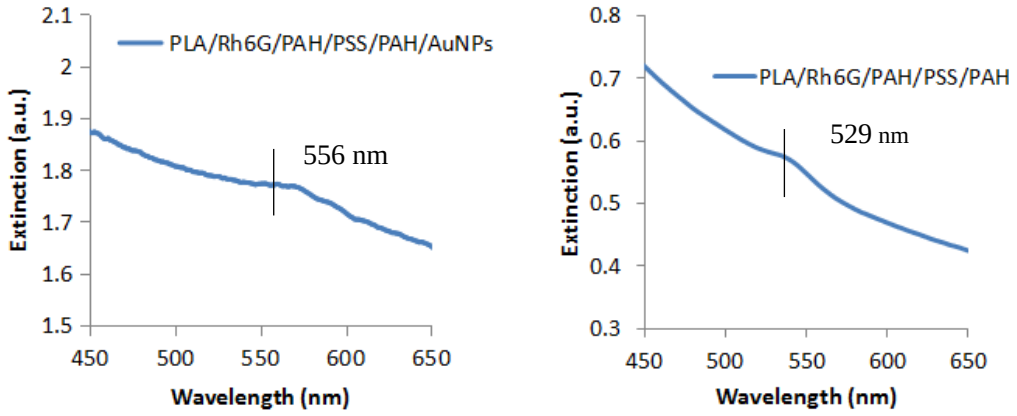

(a) (b)

Figure 19 UV-vis extinction spectrum of (a) PLA/Rh6G/PAH/PSS/PAH/AuNPs nanocapsules, and (b) PLA/Rh6G/PAH/PSS/PAH nanocapsules.

Before coating gold nanoparticles on these nanocapsules, the spectrum of PLA/Rhodamine 6G/PAH/PSS/PAH/AuNPs nanocapsules shown in Figure 19(b) was due to photo absorption by Rhodamine 6G. After coating gold nanoparticles on these nanocapsules, an obvious spectroscopic feature of metal nanoparticles, surface plasmon resonance, was observed in Figure 19(a). The wavelength of absorption peak changed from 529 nm to 556 nm. Compared to the absorption peak in pure gold nanoparticles solution (519 nm), this shift feature appeared due to the surface plasmon resonance of gold nanoparticles. When the particles are coupling, the conducting electrons which are near individual nanoparticle surfaces are shared amongst neighboring nanoparticles. This allows the surface plasmon resonance shifts to lower energies, leading the absorption peaks to red-shift to longer wavelengths [164]. In addition, the absorption wavelength of Rhodamine 6G (526 nm) is not visible here as it overlaps with strong scattering of large nanocapsules. The slope feature was due to scattering. In this study, some nanocapsules were aggregated in solution, which may produce scattering.

At each coating process, the sample needed to go through centrifugation, and this

caused materials loss (both free Rhodamine 6G dye and few nanocapsules). The nanocapsules density will be different in coating processes due to different dissolutions, thus the optical density value will be different.

In theory, the percentage of absorption or scatter from the extinction spectrum relies on the shape, size, composition, and aggregation state of a sample. Usually smaller particles have higher percentage of their extinction attributed to absorption. Therefore, when the nanocapsules are small, the scatter can be negligible, and the sample absorbs strongly. After layer-by-layer process on the nanocapsules, the capsules became larger, and the scatter affects the UV-vis measurement.

After coating with the final PAH layer, the PLA/Rhodamine 6G/PAH/PSS/PAH/AuNPs/PAH nanocapsule sample (1 mL) was collected for UV-vis measurement again, and the spectrum is shown in Figure 20.

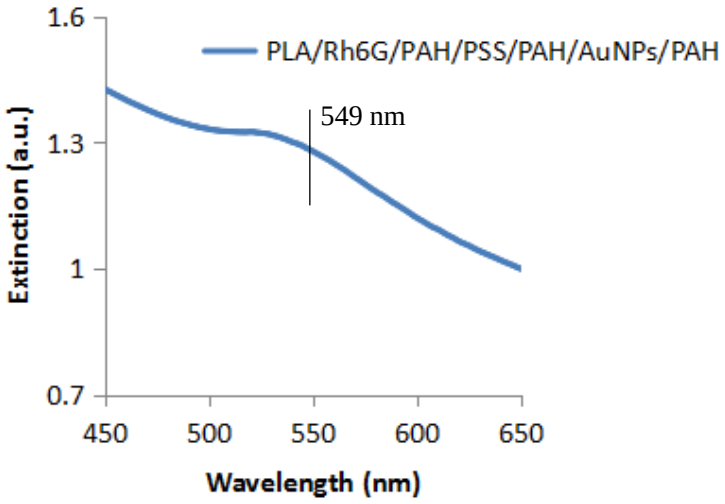

Figure 20 Extinction spectrum of PLA/Rh6G/PAH/PSS/PAH/AuNPs/PAH nanocapsules.

A similar feature as found in Figure 19 can be seen in Figure 20, apart from a light shift of absorption band to 549 nm, possibly due to a small amount of gold

nanoparticle loss caused by the centrifugation before adding PAH layer that modifies the surface plasmon band.

The fluorescence spectrum of the PLA/Rhodamine 6G/PAH/PSS/PAH/AuNPs/PAH nanocapsule sample (1 mL) is shown in Figure 21.

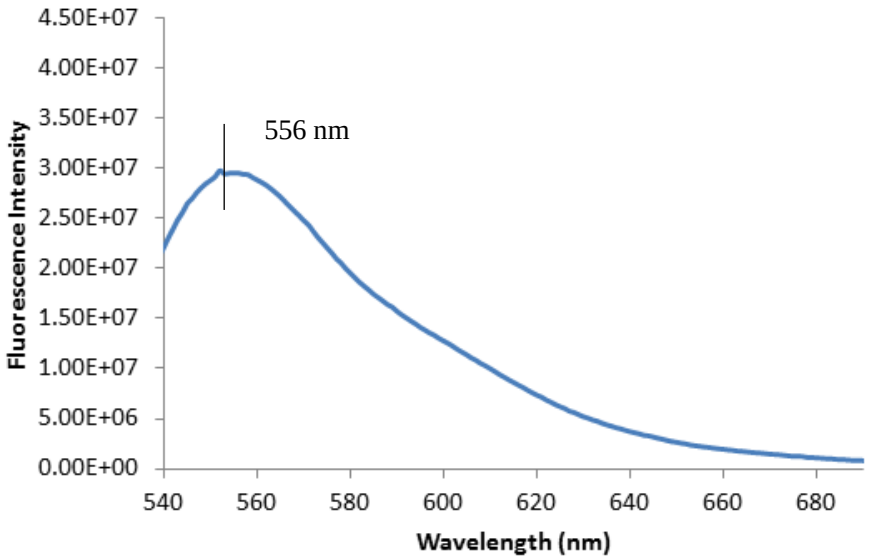

Figure 21 Fluorescence spectrum of PLA/Rh6G/PAH/PSS/PAH/AuNPs/PAH capsules (with gold nanoparticles). Excitation 526 nm.

Fluorescence spectrometry is an effective method to determine the concentration of an analyte in solution, based on its fluorescent intensity. Rhodamine 6G contained in the PLA/Rhodamine 6G/PAH/PSS/PAH/AuNPs/PAH nanocapsules displays a strong fluorescence emission. Because of this significant feature, it is one of the most widely used laser dyes in research. Figure 21 displays a typical Rhodamine 6G fluorescence emission at 556 nm, indicating the existence of Rhodamine 6G in nanocapsules. Additionally, the nanocapsules without AuNPs coating were also synthesized as a control sample to compare with the nanocapsules with AuNPs coating in this research. The fluorescence emission spectrum of the control sample

(PLA/Rhodamine 6G/PAH/PSS/PAH/PSS nanocapsules, 1mL) is shown in Figure 22.

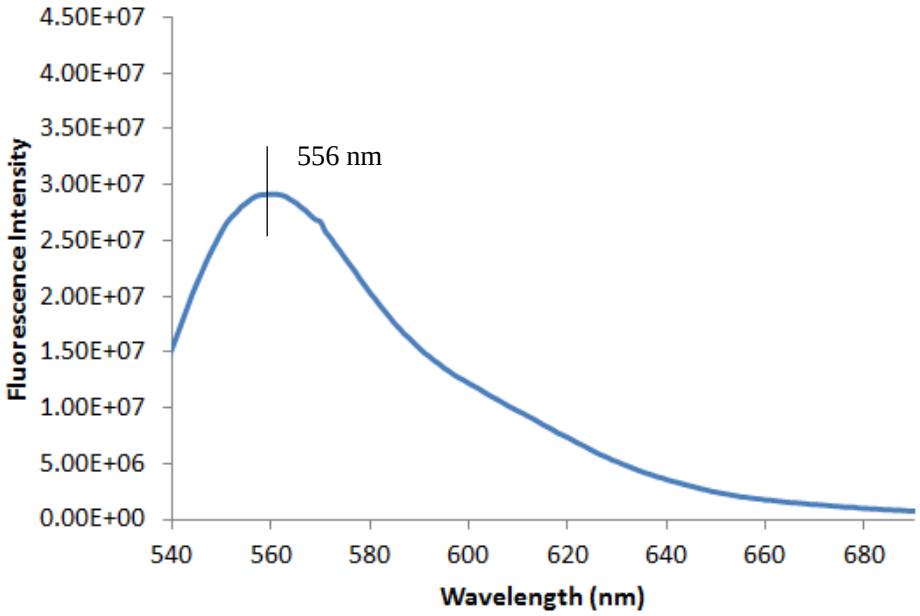

Figure 22 Fluorescence spectrum of a control sample (PLA/Rh6G/PAH/PSS/PAH/PSS capsules, without gold nanoparticles). Excitation 526 nm.

Figure 22 shows a fluorescence emission peak at 556 nm with a similar fluorescence intensity in comparison in Figure 21. It is evident that Rhodamine 6G presents in the control sample. The experimental sample and control sample had similar capsule concentrations and the same conditions for capturing spectrum.

3.4 Ultrasonic stimulation of the nanocapsules

In this research, the PLA/Rhodamine 6G/PAH/PSS/PAH/AuNPs/PAH nanocapsules and PLA/Rhodamine 6G/PAH/PSS/PAH/PSS nanocapsules (control sample), respectively suspended in distilled water (1.5 mL), were treated with ultrasonic stimulation at room temperature. The release of Rhodamine 6G dye from the

nanocapsules was examined via the fluorescence intensity change in the florescence emission spectra taken of the supernatants. For example, if the dye is released from the nanocapsules into the aqueous solution, the fluorescence emission intensity increases as the concentration of Rhodamine 6G in supernatant increases. Both the samples and control samples (nanocapsules without gold nanoparticles) underwent ultrasonic stimulation at three different duty cycles. The frequency provided from the medical device was 1 MHz, and the duty cycle employed includes low level (30% duty cycle, 0.75 W/cm^2), medium level (40% duty cycle, 1 W/cm^2), and high level (50% duty cycle, 1.2 W/cm^2). Figure 23 shows the fluorescence intensity change of dye released from PLA/dye/PAH/PSS/PAH/AuNPs/PAH nanocapsules against different ultrasonic stimulation times at three different duty cycles. The measurement was taken after each 15 minutes' stimulation.

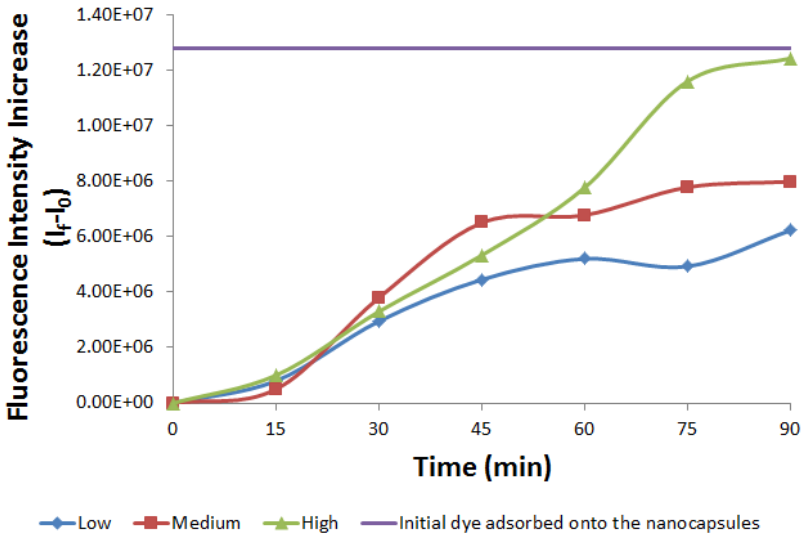

Figure 23 Fluorescence intensity of dye release from the nanocapsules with gold nanoparticles against ultrasonic stimulation time of different duty cycles. The purple line represents the total fluorescence intensity of Rh6G contained in the nanocapsules. Before experiments, the nanocapsules solution prepared for ultrasonic treatment was monitored by fluorescence measurement, to acquire the initial dye intensity adsorbed onto the nanocapsules. Upon ultrasonic stimulation with one specific duty cycle, the same sample was used throughout the experiment. After each fluorescence measurement, the supernatant was returned back to the nanocapsules container for the next 15 minutes of ultrasonic stimulation.

Fluorescence measurements showed that samples after high-duty cycle ultrasonic treatment for 6 times (90 minutes) released more of the dye than that under medium or low-duty cycle treatment. Little dye was released from these nanocapsules after the first 15 minutes of treatment. Clear increases of fluorescence intensities were observed after the second stimulation, although no significant differences were found among different duty cycles. With the increase of ultrasonic stimulation times, the fluorescence intensity further increased. It indicates that the ultrasonic treatment promotes the dye release from nanocapsules with gold nanoparticles. After the fourth (total 60 minutes) ultrasonic treatment, the dye was still released from samples. However, the rate of fluorescence intensity changes reduced, particularly for medium and low-duty cycle treatments. After the sixth ultrasonic stimulation (90 minutes), the fluorescence intensity of dye released from sample under high-duty cycle treatment was close to the initial total intensity of dye adsorbed onto the nanocapsules. It implies that most of the dye contained in samples had been released. In comparison, the fluorescence intensities of dye released from samples with medium or low-duty cycle of ultrasound were lower than that with high-duty cycle. This means that there was still dye in the nanocapsules. It might be expected that ultrasound with medium or low-duty cycle would have weaker intensity than the high duty cycle, causing less release of dye from the nanocapsules. Nevertheless, the dye release from the nanocapsules with ultrasonic stimulation was present. After 45 minutes of treatment, more dye was released from nanocapsules upon medium duty cycle of ultrasound than those upon high duty cycle was noticed. It requires more experiments to confirm the reasons, exploring the mechanism of this phenomenon.

To study the influence of the presence of the gold nanoparticles on the efficiency of dye release, nanocapsules without gold nanoparticles in their shells were also synthesized and analyzed. Their results are shown in Figure 24.

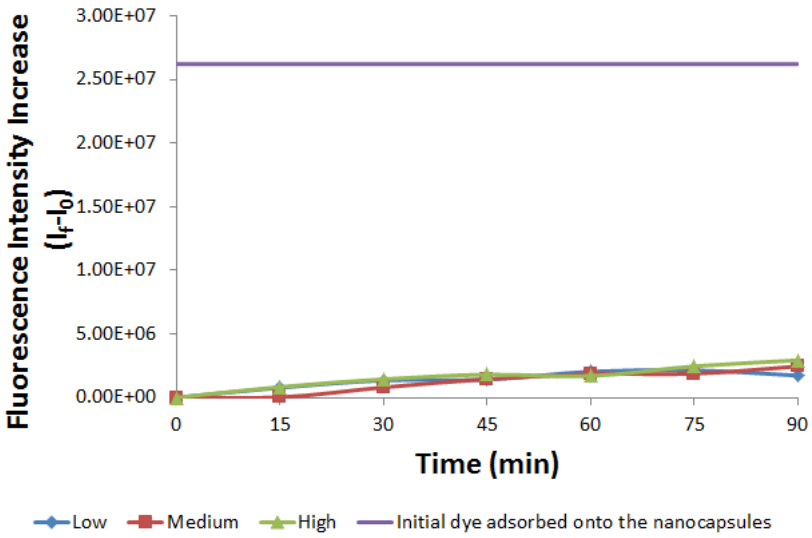

Figure 24 Fluorescence intensity of dye release from the nanocapsules without gold nanoparticles measured after various ultrasonic stimulation times of different duty-cycles. The purple line represents the emission intensity of Rh6G contained in the nanocapsules without gold nanoparticles. Before experiments, the nanocapsules solution prepared for ultrasonic treatment was monitored by fluorescence measurement, to acquire the initial dye intensity adsorbed onto the nanocapsules. Upon ultrasonic stimulation with one specific duty cycle, the same sample was used throughout the experiment. After each fluorescence measurement, the supernatant was returned back to the nanocapsules container for the next 15 minutes of ultrasonic stimulation.

After the first ultrasonic stimulation, there was almost no dye released from the nanocapsules without gold nanoparticles. The release of dye from samples was observable after the second stimulation. However, the change of fluorescence intensity as the increase of ultrasonic treatment time was small. After 6 treatments, the fluorescence intensity was just 10% of the total initial fluorescence intensity. Moreover, there was no significant difference on the efficiency of dye release by employing different duty cycles. It is thus clear that gold nanoparticles in nanocapsule play an important role in the ultrasonic induced release of dye.

Finally, the release of dye from samples (1.5 mL) stored in room temperature without ultrasonic treatment for four weeks was also studied as a comparison. Both nanocapsules with and without gold nanoparticles were used in this study. Figure 25 shows fluorescence intensity changes of dye released from nanocapsules after long

time storage at room temperature.

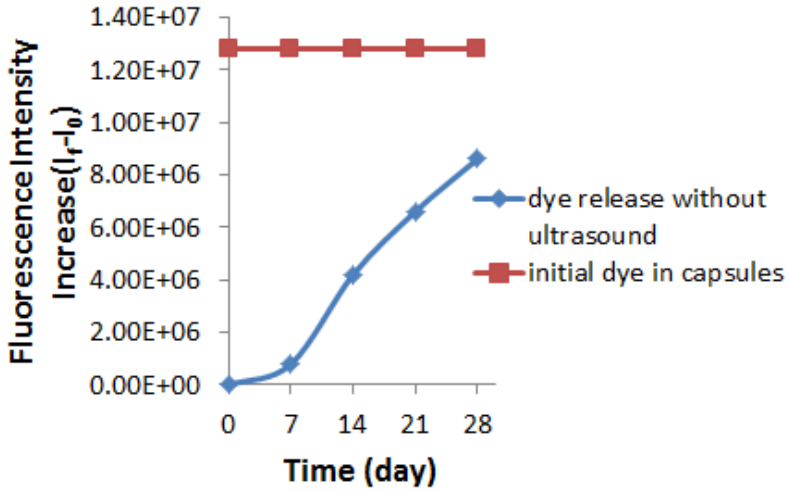

(a)

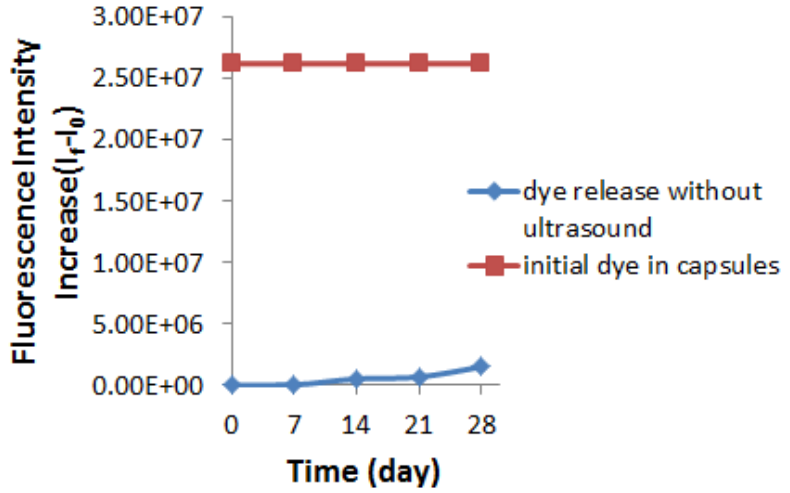

(b)

Figure 25 Fluorescence intensity of dye released from nanocapsules (a) with (PLA/Rh6G/PAH/PSS/PAH/AuNPs/PAH nanocapsules) and (b) without (PLA/Rh6G/PAH/PSS/PAH/PSS nanocapsules) gold nanoparticles after room temperature storage (without any ultrasonic stimulation). The red line represents the emission intensity of Rh6G contained in the samples.

Figure 25 (a) shows that after an initial small release in the first week, large amount of dye released from nanocapsules with gold nanoparticles in the following three weeks. In contrast, no obvious changes in the fluorescence intensity was observed in the case of nanocapsules without gold nanoparticles for the first weeks. The intensity of released dye after 4 weeks was significantly weak compared to that from nanocapsule with gold nanoparticles. This finding suggests that nanocapsules containing gold nanoparticles are less stable compared to those without gold nanoparticles. It is not clear whether this is related to the thermal effect from gold nanoparticles under laser illumination or due to centrifugation. Laser illumination or centrifugation may produce heat, and this heating could affect the permeability of nanocapsules shell and cause a dye release. Further study is required to reveal the mechanism. Nevertheless, it is clear that dye release in the first week was weak for both samples. As the ultrasonic treatment was completed within 1-2 days, the influence of "natural" release of dye on the results in Figure 23 and 24 was negligible.

3.5 Discussion - Effect of the dye release from nanocapsules

The effects of ultrasound as a release trigger may be attributed to acoustic cavitation in liquids under ultrasonic vibrations with a frequency of more than 20 kHz. As demonstrated by Maria N. Antipina et al., ultrasound energy produces pressure and can cause the shrinkage of gas-filled nanobubbles. Then, the cavitating nanobubbles implode, which produces local shock waves, destroying the nanocapsule assemblies [165-169]. Even at low input power, the collapse of microbubbles in liquids results in an enormous concentration of energy. When the capsules are subjected to ultrasonic stimulation, shear forces between the successive fluid layers occurs, which leads to the disruption of the capsule assemblies and the subsequent release of their payloads [165]. Therefore, acoustic cavitation resulting in dye release from the nanocapsules

in this study is a possible factor.

In previous research, employment of ultrasonic stimulation for opening polyelectrolyte nanocapsules was studied by using PSS/PAH composed layers [166-169]. Among those, the performance of $CaCO_3$ microcapsules assembled with polyelectrolyte layers and gold nanoparticles were studied by using ultrasonic stimulation for different durations, and the ultrasound employed was at the frequency of 20 kHz, and 120 W of power output. When the ultrasonic stimulation was performed for 10 s, nearly all of the microcapsules were disrupted. However, for shorter ultrasonic stimulation times, the microcapsules seem mechanically more stable when gold nanoparticles are contained in the shell. The results indicate that the stability of microcapsules depends on the duration of ultrasonic stimulation. In the present research, after the sixth ultrasonic stimulation (90 minutes), most of the dye contained in the nanocapsules with gold shells had been released under high-duty cycle treatment.

In this case of nanocapsules, the polymeric shell plays a significant role in protecting the payload incorporated and in the payload release profile [170-171]. As reported, the thickness value of polycation or polyanion is between 1.5 and 1.7 nm in dry state [172-173]. The shell thickness of nanocapsules prepared by the layer-by-layer technique depends on the number of layers. The influence of polymer thickness on the drug release was illustrated by Balakrishnan et al. [174]. Drug release from thinner coatings carrier was reported to be fast initially but subject to a rapid decline when compared to a thicker polymer coatings carrier. According to previous research, when the membrane thickness is increased, the diffusional path length of a drug molecule through the membrane will increase, thus reducing the rate of drug release [175]. In other words, the thickness of the composite film may influence the permeability of the carrier shell. When the thickness of nanocapsules is increased, more intense ultrasonic stimulation should be employed to achieve drug delivery

from the nanocapsules.

In this study, the presence of gold nanoparticles allowed the dye to be released from PLA/dye/PAH/PSS/PAH/AuNPs/PAH nanocapsules more efficiently, compared to those nanocapsules without gold nanoparticles. According to the results, several factors may play a role in the stimulation process. The presence of gold nanoparticles in the PLA/dye/PAH/PSS/PAH/AuNPs/PAH nanocapsules makes the shells stiffer and lowers their elasticity, which may have an effect on how easily the shells are moved upon employing an oscillating force to them in liquid by ultrasonic stimulation. If they are moved, rupturing may occur as expected. As illustrated by Fery et al., the presence of inorganic nanoparticles increases the density contrast (differences in density of the shells) of a microcapsule shell, which also decreases the elasticity of the shell. These are important to achieve high efficiency of the ultrasonically treated release of compounds encapsulated in capsules [176]. Furthermore, both ZnO-containing capsules and capsules without ZnO nanoparticles have been investigated with ultrasonic treatment by Tatiana A. Kolesnikova et al. The results indicate that the incorporation of ZnO nanoparticles increases the density contrast of capsules' shell, and allows the shells to be stiffer, and improves the absorption of acoustic energy [169]. As for the nanocapsules without gold nanoparticles, they presented little dye release in this research. It can be assumed that the capsules may be disrupted because of the absorption of intense ultrasound energy over a longer time. In previous research, ultrasonic stimulation operating on the capsules has been proven to produce heat. High temperature causes changes in permeability of the outer shell and can even rupture the capsules. Subsequently, the release of capsules payload will be achieved [177]. The heat produced by ultrasound may also have an influence on the dye released from samples without gold nanoparticles.

Additionally, the size of gold nanoparticles coated on nanocapsules may also have

influences on the efficiency of dye release from nanocapsules, but there is not much research on the details. Compared to larger gold nanoparticles employed in the same proportion, smaller gold nanoparticles coated on the nanocapsules may cause a higher density on the shell, thus lowering the elasticity of the shell and improving the efficient release of drug from the nanocapsules. The effects caused by nanoparticle size should be further studied in future.

The fabrication process of the capsules would therefore need improvement in future research. By comparison, in the case without any ultrasonic stimulation, dye was still released from capsules with and without gold nanoparticles at room temperature, after a few days; it seems that the capsules are not stable over long periods of time. As illustrated by Shchukin et al., the effect of ultrasonic stimulation on the release of temperature treated Fe_3O_4/polyelectrolyte capsules was studied. The findings indicate that the heated capsules are more stable under ultrasonic treatment than initial ones [166].

The sensitivity of nanocapsules to ultrasonic stimulation relies on the stiffness and elasticity of the shells, which can be tuned to work in medical conditions. Therefore, the application of ultrasonic stimulation as a remote treatment to induce the payload release from capsules may have good potential outlook with further improvement in the stability and sensitivity to the external stimulus.

Chapter 4: Conclusions and future work

This thesis aims to investigate a drug delivery system with stimuli-responsive polymeric nanocapsules that achieve locally controlled drug release by remote ultrasonic stimulation. The nanocapsules were synthesized with polyelectrolyte layers and gold nanoparticles by using a layer-by-layer assembly technique, encapsulated with a model dye used in place of anti-restenotic drugs. The nanocapsules with and without gold nanoparticles embedded in the shell were examined for the response to ultrasonic stimulation, demonstrating that in both cases, the dye release was observed after six cycles of stimulation. The presence of gold nanoparticles significantly enhances the efficiency of the ultrasonically induced dye release from the nanocapsules. In particular, after the sixth ultrasonic stimulation (90 mins), the fluorescence intensity of the dye released from the sample with gold nanoparticles under high-duty cycle treatment was close to the initial total intensity of dye adsorbed onto the nanocapsules. However, in the case of nanocapsules without gold nanoparticles, the change of fluorescence intensity with increasing ultrasonic treatment time was weak. As a comparison in the case of absence of ultrasonic treatment, the nanocapsules containing gold nanoparticles are less stable compared to those without gold nanoparticles after extended storage at room temperature. After four weeks, there was much more dye released from the capsules with gold nanoparticles than that of capsules without gold nanoparticles.

The observation of dye release from the nanocapsules with gold nanoparticles upon ultrasonic stimulation demonstrates the potential in medical applications, as it presents a potential outlook for the remotely controlled release of a drug in specific sites, decreasing the potential negative effects on healthy tissue.

In this research, the trigger mechanism was remotely stimulated with ultrasound at a frequency of 1MHz, which poses no harm for the human body. In the future, these drug-loaded nanocapsules will be applied onto stents, allowing for a stimuli-response

to ultrasound. As for the clinical application, nanocapsules are usually placed specifically to achieve controllable drug release within a few days, which can prevent in-stent restenosis.

In this research, the mechanism of ultrasonic stimulation that worked on nanocapsules was not clear, and needs further research. Previously, the effect of ultrasonic irradiation on Fe_3O_4-containing polyelectrolyte capsules was demonstrated by Dmitry G et al., [169]. Ultrasonic treatment results in the complete destruction of the capsule shell, and the size of the shell residues depends on the intensity of the acoustic waves. In future research, the nanocapsules should be investigated by transmission electron microscopy, or laser scanning confocal microscopy upon ultrasonic treatment, with different power and intensity to determine the mechanism of ultrasound worked on nanocapsules disruption. In this study, the model dye served as a tracer material in place of anti-restenotic drugs. In order to employ the drug-containing nanocapsules in the treatment of cardiovascular disease, drugs such as paclitaxel or rapamycin could be applied in further experiments. The release properties of Rhodamine 6G and drugs such as these may be different upon ultrasonic stimulation, and therefore there is a need for further research.

The effect of different duty cycles of ultrasound used in the first few times of stimulation presented no significant differences, and the maximum duty cycle in this experiment was 5/10 cycle (5 s pulse/ 10 s pause). In further experiments a higher cycle (such as 1/1 cycle) should be used to detect the clear differences of duty cycle of ultrasound on nanocapsules' treatment. Additionally, a range of frequencies should be adopted to study the effect on the drug release properties of nanocapsules.

The number of layers coated on the nanocapsules should be considered as a factor which may have impact on the drug release properties upon ultrasound in future. The drug release profile can be significantly influenced by the structure of the nanocapsules themselves. In previous research, the minimum number of capsule

layers required for stability is ten, with an optimum of fourteen to sixteen, with any more layers rendering the microcapsules unstable. As more layers increase the microcapsule thickness, it may need more energy derived from ultrasonic treatment to destroy the shells [178]. Furthermore, the size and proportion of metal nanoparticles contained in the nanocapsules should be increased, and the effect of this on the drug release process is another area that requires further research.

There is an absence of research when considering the clinically relevant conditions, such as dose of drug and biodegradation of residue nanocapsules. Thus, this aspect of medicine is still in its early stage, and it requires much study for development to achieve a clinically viable drug delivery system.

The nanocapsules containing gold nanoparticles in this research showed more sensitivity to ultrasound stimulation. Capsules containing other metal nanoparticles such as magnetic particles may give rise to different results upon ultrasonic treatment. Additionally, nanocapsules containing magnetite nanoparticles can be concentrated by an external magnet. This property may help the nanocapsules to reach a specific site easily. Therefore, the efficiency of drug release from nanocapsules upon ultrasonic stimulation could be improved.

Further studies on the effect of nanocapsules composite, ultrasonic frequency and duty cycles on remotely controlled drug release will provide insights into the potential and application of the nanocapsule drug delivery system in treating in-stent restenosis.

References

[1] Mohamed, F., & van der Walle, C. F. (2008). Engineering biodegradable polyester particles with specific drug targeting and drug release properties.Journal of pharmaceutical sciences, 97(1), 71-87.

[2] Alwan, A. (2011). *Global status report on noncommunicable diseases 2010*. World Health Organization.

[3] Ito, S., Nakasuka, K., Sekimoto, S., Miyata, K., Inomata, M., Yoshida, T., ... & Sato, K. (2012). Intracoronary Imaging and Histopathology of Late Phase In-Stent Restenosis after Coronary Stent Implantation. *ISRN Vascular Medicine*, *2012*.

[4] Kiran, U., & Makhija, N. (2009). Patient with recent coronary artery stent requiring major non cardiac surgery. *Indian journal of anaesthesia*, *53*(5), 582.

[5] Ma, W. J., Yuan, X. B., Kang, C. S., Su, T., Yuan, X. Y., Pu, P. Y., & Sheng, J. (2008). Evaluation of blood circulation of polysaccharide surface-decorated PLA nanoparticles. *Carbohydrate Polymers*, *72*(1), 75-81.

[6] Reed, A. M., & Gilding, D. K. (1981). Biodegradable polymers for use in surgery—poly (glycolic)/poly (lactic acid) homo and copolymers: 2. *In vitro* degradation. *Polymer*, *22*(4), 494-498.

[7] Anderson, J. M., & Shive, M. S. (2012). Biodegradation and biocompatibility of PLA and PLGA microspheres. *Advanced drug delivery reviews*, *64*, 72-82.

[8] Liu, H. L., McDannold, N., & Hynynen, K. (2005). Focal beam distortion and treatment planning in abdominal focused ultrasound surgery. Medical physics, 32(5), 1270-1280.

[9] Skirtach, A. G., De Geest, B. G., Mamedov, A., Antipov, A. A., Kotov, N. A., & Sukhorukov, G. B. (2007). Ultrasound stimulated release and catalysis using polyelectrolyte multilayer capsules. *Journal of materials chemistry, 17*(11), 1050-1054.

[10] Rapoport, N. (1999). Stabilization and activation of Pluronic micelles for tumor-targeted drug delivery. *Colloids and Surfaces B: Biointerfaces*, *16*(1), 93-111.

[11] Husseini, G. A., Myrup, G. D., Pitt, W. G., Christensen, D. A., & Rapoport, N. Y. (2000). Factors affecting acoustically triggered release of drugs from polymeric micelles. *Journal of Controlled Release*, *69*(1), 43-52.

[12] Marin, A., Sun, H., Husseini, G. A., Pitt, W. G., Christensen, D. A., & Rapoport, N. Y. (2002). Drug delivery in pluronic micelles: effect of high-frequency ultrasound on drug release from micelles and intracellular uptake.*Journal of Controlled Release*, *84*(1), 39-47.

[13] Smith, M. J., Eccleston, M. E., & Slater, N. K. (2008). The effect of high intensity focussed ultrasound (HIFU) on pH responsive PEGylated micelles.*Journal of the Acoustical Society of America*, *123*(5), 3223.

[14] Zeng, Y., & Pitt, W. G. (2006). A polymeric micelle system with a hydrolysable segment for drug delivery. *Journal of Biomaterials Science, Polymer Edition*, *17*(5), 591-604.

[15] Johnston, A. P., Such, G. K., & Caruso, F. (2010). Triggering release of encapsulated cargo. *Angewandte Chemie International Edition, 49*(15), 2664-2666.

[16] Lin, H. Y., & Thomas, J. L. (2003). PEG-lipids and oligo (ethylene glycol) surfactants enhance the ultrasonic permeabilizability of liposomes.*Langmuir*, *19*(4), 1098-1105.

[17] Chen, Z. Y., Lin, Y., Yang, F., Jiang, L., & ping Ge, S. (2013). Gene therapy for cardiovascular disease mediated by ultrasound and microbubbles.*Cardiovascular ultrasound*, *11*(1), 1.

[18] Mohan, S., & Dhall, A. (2010). A comparative study of restenosis rates in bare metal and drug-eluting stents. *International Journal of Angiology, 19*(02), e66-e72.

[19] Alfonso, F., Byrne, R. A., Rivero, F., & Kastrati, A. (2014). Current treatment of in-stent restenosis. *Journal of the American College of Cardiology*, *63*(24), 2659-2673.

[20] Jonas, S., Goldsteen, R. L., & Goldsteen, K. (2007). *An introduction to the US health care system*. Springer Publishing Company.

[21] Dangas, G., & Kuepper, F. (2002). Restenosis: Repeat narrowing of a coronary artery prevention and treatment. *Circulation*, 105(22), 2586-2587.

[22] Regar, E., Sianos, G., & Serruys, P. W. (2001). Stent development and local drug delivey. *British medical bulletin, 59*(1), 227-248.

[23] Lansky, A. J., Costa, R. A., Mintz, G. S., Tsuchiya, Y., Midei, M., Cox, D. A., ... & Farah, A. (2004). Non–Polymer-Based Paclitaxel-Coated Coronary Stents for the Treatment of Patients With De Novo Coronary Lesions Angiographic Follow-Up of the DELIVER Clinical Trial. *Circulation*, *109*(16), 1948-1954.

[24] Morice, M. C., Serruys, P. W., Sousa, J. E., Fajadet, J., Ban Hayashi, E., Perin, M., ... & Molnar, F. (2002). A randomized comparison of a sirolimus-eluting stent with a standard stent for coronary revascularization. *New England Journal of Medicine*, *346*(23), 1773-1780.

[25] Moses, J. W., Leon, M. B., Popma, J. J., Fitzgerald, P. J., Holmes, D. R., O'Shaughnessy, C., ... & Jaeger, J. L. (2003). Sirolimus-eluting stents versus standard stents in patients with stenosis in a native coronary artery.*New England Journal of Medicine*, *349*(14), 1315-1323.

[26] Lee, E. S., Na, K., & Bae, Y. H. (2005). Super pH-sensitive multifunctional polymeric micelle. *Nano letters, 5*(2), 325-329.

[27] Gingras, A. C., Raught, B., & Sonenberg, N. (2004). mTOR signaling to translation. In *TOR* (pp. 169-197). Springer Berlin Heidelberg.

[28] Giannakakou, P., Robey, R., Fojo, T., & Blagosklonny, M. V. (2001). Low concentrations of paclitaxel induce cell type-dependent p53, p21 and G1/G2 arrest instead of mitotic arrest: molecular determinants of paclitaxel-induced cytotoxicity. *Oncogene*, *20*(29), 3806-3813.

[29] García-García, H. M., Vaina, S., Tsuchida, K., & Serruys, P. W. (2006). Drug-eluting stents. *Archivos de cardiologia de Mexico*, *76*(3), 297.

[30] Couvreur, P., & Vauthier, C. (2006). Nanotechnology: intelligent design to treat complex disease. *Pharmaceutical research*, *23*(7), 1417-1450.

[31] Torchilin, V. P. (2007). Targeted pharmaceutical nanocarriers for cancer therapy and imaging. *The AAPS journal*, *9*(2), E128-E147.

[32] Orive, G., Anitua, E., Pedraz, J. L., & Emerich, D. F. (2009). Biomaterials for promoting brain protection, repair and regeneration. *Nature Reviews Neuroscience*, *10*(9), 682-692.

[33] Shenoy, D., Little, S., Langer, R., & Amiji, M. (2005). Poly (ethylene oxide)-modified poly (β-amino ester) nanoparticles as a pH-sensitive system for tumor-targeted delivery of hydrophobic drugs. 1. *In vitro* evaluations. *Molecular pharmaceutics, 2*(5), 357-366.

[34] Shenoy, D., Little, S., Langer, R., & Amiji, M. (2005). Poly (ethylene oxide)-modified poly

(β-amino ester) nanoparticles as a pH-sensitive system for tumor-targeted delivery of hydrophobic drugs: part 2. *In vivo* distribution and tumor localization studies. *Pharmaceutical research*, *22*(12), 2107-2114.

[35] Shenoy, D. B., & Amiji, M. M. (2005). Poly (ethylene oxide)-modified poly (ε-caprolactone) nanoparticles for targeted delivery of tamoxifen in breast cancer. *International journal of pharmaceutics*, *293*(1), 261-270.

[36] Kommareddy, S., & Amiji, M. (2005). Preparation and evaluation of thiol-modified gelatin nanoparticles for intracellular DNA delivery in response to glutathione. *Bioconjugate chemistry*, *16*(6), 1423-1432.

[37] Vaupel, P., Kallinowski, F., & Okunieff, P. (1989). Blood flow, oxygen and nutrient supply, and metabolic microenvironment of human tumors: a review.*Cancer research*, *49*(23), 6449-6465.

[38] Sukhishvili, S. A. (2005). Responsive polymer films and capsules via layer-by-layer assembly. *Current Opinion in Colloid & Interface Science*, *10*(1), 37-44.

[39] Inoue, H., Sato, K., & Anzai, J. I. (2005). Disintegration of layer-by-layer assemblies composed of 2-iminobiotin-labeled poly (ethyleneimine) and avidin. *Biomacromolecules*, *6*(1), 27-29.

[40] Meyer, D. E., Shin, B. C., Kong, G. A., Dewhirst, M. W., & Chilkoti, A. (2001). Drug targeting using thermally responsive polymers and local hyperthermia. *Journal of controlled release*, *74*(1), 213-224.

[41] Saito, G., Swanson, J. A., & Lee, K. D. (2003). Drug delivery strategy utilizing conjugation via reversible disulfide linkages: role and site of cellular reducing activities. *Advanced drug delivery reviews*, *55*(2), 199-215.

[42] Arruebo, M., Fernández-Pacheco, R., Ibarra, M. R., & Santamaría, J. (2007). Magnetic nanoparticles for drug delivery. *Nano today*, *2*(3), 22-32.

[43] Gould, P. (2006). Nanomagnetism shows *in vivo* potential. *Nano Today*, *1*(4), 34-39.

[44] Ito, A., Shinkai, M., Honda, H., & Kobayashi, T. (2005). Medical application of functionalized magnetic nanoparticles. *Journal of bioscience and bioengineering*, *100*(1), 1-11.

[45] Rapoport, N. (2004). Combined cancer therapy by micellar-encapsulated drug and ultrasound. *International journal of pharmaceutics*, *277*(1), 155-162.

[46] Klibanov, A. L. (2006). Microbubble contrast agents: targeted ultrasound imaging and ultrasound-assisted drug-delivery applications. *Investigative radiology, 41*(3), 354-362.

[47] Gao, Z. G., Fain, H. D., & Rapoport, N. (2005). Controlled and targeted tumor chemotherapy by micellar-encapsulated drug and ultrasound. *Journal of Controlled Release*, *102*(1), 203-222.

[48] Rapoport, N. (2007). Physical stimuli-responsive polymeric micelles for anti-cancer drug delivery. *Progress in Polymer Science*, *32*(8), 962-990.

[49] Angelatos, A. S., Radt, B., & Caruso, F. (2005). Light-responsive polyelectrolyte/gold nanoparticle microcapsules. *The Journal of Physical Chemistry B*, *109*(7), 3071-3076.

[50] Sukhishvili, S. A. (2005). Responsive polymer films and capsules via layer-by-layer assembly. *Current Opinion in Colloid & Interface Science*, *10*(1), 37-44.

[51] Skirtach, A. G., Antipov, A. A., Shchukin, D. G., & Sukhorukov, G. B. (2004). Remote activation of capsules containing Ag nanoparticles and IR dye by laser light. *Langmuir*, *20*(17), 6988-6992.

[52] Radi, B., Smith, T. A., & Caruso, F. (2004). Optically addressable nanostructured capsules. *Advanced Materials, 16*(23-24), 2184-2189.

[53] Kost, J., & Langer, R. (1992). Responsive polymer systems for controlled delivery of therapeutics. *Trends in biotechnology*, *10*, 127-131.

[54] Zhao, Y. Z., Du, L. N., Lu, C. T., Jin, Y. G., & Ge, S. P. (2013). Potential and problems in ultrasound-responsive drug delivery systems. *Int J Nanomedicine*, *8*, 1621-1633.

[55] Marmottant, P., & Hilgenfeldt, S. (2003). Controlled vesicle deformation and lysis by single oscillating bubbles. *Nature, 423*(6963), 153-156.

[56] Norris, P., Noble, M., Francolini, I., Vinogradov, A. M., Stewart, P. S., Ratner, B. D., ... & Stoodley, P. (2005). Ultrasonically controlled release of ciprofloxacin from self-assembled coatings on poly (2-hydroxyethyl methacrylate) hydrogels for Pseudomonas aeruginosa biofilm prevention.*Antimicrobial agents and chemotherapy*, *49*(10), 4272-4279.

[57] Lentacker, I., De Geest, B. G., Vandenbroucke, R. E., Peeters, L., Demeester, J., De Smedt, S. C., & Sanders, N. N. (2006). Ultrasound-responsive polymer-coated microbubbles that bind and protect DNA.*Langmuir*, *22*(17), 7273-7278.

[58] Marmottant, P., & Hilgenfeldt, S. (2003). Controlled vesicle deformation and lysis by single oscillating bubbles. *Nature*, *423*(6936), 153-156.

[59] Kost, J., Leong, K., & Langer, R. (1989). Ultrasound-enhanced polymer degradation and release of incorporated substances. *Proceedings of the National Academy of Sciences*, *86*(20), 7663-7666.

[60] Kost, J., Leong, K., & Langer, R. (1986). Ultrasonic modulated drug delivery systems. In *Polymers in Medicine II* (pp. 387-396). Springer US.

[61] Lavon, I., & Kost, J. (1998). Mass transport enhancement by ultrasound in non-degradable polymeric controlled release systems. *Journal of Controlled Release*, *54*(1), 1-7.

[62] Liu, L. S., Kost, J., D'Emanuele, A., & Langer, R. (1992). Experimental approach to elucidate the mechanism of ultrasound-enhanced polymer erosion and release of incorporated substances. *Macromolecules*, *25*(1), 123-128.

[63] Kost, J., Leong, K., & Langer, R. (1988, June). Ultrasonically controlled polymeric drug delivery. In *Makromolekulare Chemie. Macromolecular Symposia* (Vol. 19, No. 1, pp. 275-285). Hüthig & Wepf Verlag.

[64] Kost, J., Liu, L. S., Gabelnick, H., & Langer, R. (1994). Ultrasound as a potential trigger to terminate the activity of contraceptive delivery implants.*Journal of controlled release*, *30*(1), 77-81.

[65] MIYAZAKI, S., YOKOUCHI, C., & TAKADA, M. (1988). External control of drug release: controlled release of insulin from a hydrophilic polymer implant by ultrasound irradiation in diabetic rats. *Journal of pharmacy and pharmacology*, *40*(10), 716-717.

[66] Miyazaki, S., Hou, W.-M., Takada, M. (1985). Controlled drug release by ultrasound irradiation. *Chemical and pharmaceutical bulletin, 33(*1), 428-431.

[67] Abbaspourrad, A., Carroll, N. J., Kim, S. H., & Weitz, D. A. (2013). Polymer microcapsules with programmable active release. *Journal of the American Chemical Society*, *135*(20), 7744-7750.

[68] Lin, H. Y., & Thomas, J. L. (2003). PEG-lipids and oligo (ethylene glycol) surfactants enhance the ultrasonic permeabilizability of liposomes.*Langmuir*, *19*(4), 1098-1105.

[69] Husseini, G. A., Myrup, G. D., Pitt, W. G., Christensen, D. A., & Rapoport, N. Y. (2000).

Factors affecting acoustically triggered release of drugs from polymeric micelles. *Journal of Controlled Release*, *69*(1), 43-52.

[70] Husseini, G. A., Rapoport, N. Y., Christensen, D. A., Pruitt, J. D., & Pitt, W. G. (2002). Kinetics of ultrasonic release of doxorubicin from pluronic P105 micelles. *Colloids and Surfaces B: Biointerfaces*, *24*(3), 253-264.

[71] Rapoport, N. Y., Herron, J. N., Pitt, W. G., & Pitina, L. (1999). Micellar delivery of doxorubicin and its paramagnetic analog, ruboxyl, to HL-60 cells: effect of micelle structure and ultrasound on the intracellular drug uptake.*Journal of Controlled Release*, *58*(2), 153-162.

[72] Nelson, J. L., Roeder, B. L., Carmen, J. C., Roloff, F., & Pitt, W. G. (2002). Ultrasonically activated chemotherapeutic drug delivery in a rat model.*Cancer research*, *62*(24), 7280-7283.

[73] Munshi, N., Rapoport, N., & Pitt, W. G. (1997). Ultrasonic activated drug delivery from Pluronic P-105 micelles. *Cancer letters*, *118*(1), 13-19.

[74] Pua, E. C., & Zhong, P. (2009). Ultrasound-mediated drug delivery. *IEEE engineering in medicine and biology magazine*, *28*(1), 64-75.

[75] Borges, J., Rodrigues, L. C., Reis, R. L., & Mano, J. F. (2014). Layer-by-layer assembly of light-responsive polymeric multilayer systems. *Advanced Functional Materials, 24*(36), 5624-5648.

[76] Khillan, R. K., Ghan, R., Dasaka, R., Su, Y., Lvov, L., & Varahramyan, K. (2004, September). Layer-by-layer nanoarchitecture of ultrathin films assembled of PEDOT-PSS and PPy to act as hole transport layer in polymer light emitting diodes and polymer transistors. In *Polymers and Adhesives in Microelectronics and Photonics, 2004. POLYTRONIC 2004. 4th IEEE International Conference on* (pp. 225-229). IEEE.

[77] Kleinfeld, E. R., & Ferguson, G. S. (1994). Stepwise formation of multilayered nanostructural films from macromolecular precursors. *Science, 265*(5170), 370-373.

[78] Keller, S. W., Kim, H. N., & Mallouk, T. E. (1994). Layer-by-Layer Assembly of intercalation compounds and heterostructures on surfaces: Toward molecular" beaker" epitaxy. *Journal of the American Chemical Society, 116*(19), 8817-8818.

[79] Lvov, Y., Ariga, K., Onda, M., Ichinose, I., & Kunitake, T. (1997). Alternate assembly of ordered multilayers of SiO2 and other nanoparticles and polyions. *Langmuir*, *13*(23), 6195-6203.

[80] Caruso, F., Caruso, R. A., & Möhwald, H. (1998). Nanoengineering of inorganic and hybrid hollow spheres by colloidal templating. *Science, 282*(5391), 1111-1114.

[81] Shchukin, D. G., Ustinovich, E. A., Sukhorukov, G. B., Möhwald, H., & Sviridov, D. V. (2005). Metallized polyelectrolyte microcapsules. *Advanced Materials*, *17*(4), 468-472.

[82] Zhang, H., Lu, H., & Hu, N. (2006). Fabrication of electroactive layer-by-layer films of myoglobin with gold nanoparticles of different sizes. *The Journal of Physical Chemistry B*, *110*(5), 2171-2179.

[83] Chirea, M., Pereira, C. M., & Silva, F. (2007). Catalytic effect of gold nanoparticles self-assembled in multilayered polyelectrolyte films. *The Journal of Physical Chemistry C*, *111*(26), 9255-9266.

[84] Srivastava, S., & Kotov, N. A. (2008). Composite layer-by-layer (LBL) assembly with inorganic nanoparticles and nanowires. *Accounts of chemical research*, *41*(12), 1831-1841.

[85] Couto, D. S., Alves, N. M., & Mano, J. F. (2009). Nanostructured multilayer coatings combining chitosan with bioactive glass nanoparticles. *Journal of nanoscience and nanotechnology*, *9*(3), 1741-1748.

[86] Andres, C. M., & Kotov, N. A. (2010). Inkjet deposition of layer-by-layer assembled films. *Journal of the American Chemical Society*, *132*(41), 14496-14502.

[87] Tettey, K. E., Ho, J. W., & Lee, D. (2011). Modulating layer-by-layer assembly of oppositely charged nanoparticles using a short amphiphilic molecule. *The Journal of Physical Chemistry C*, *115*(14), 6297-6304.

[88] Jin, H., Choi, S., Velu, R., Kim, S., & Lee, H. J. (2012). Preparation of multilayered CdSe quantum dot sensitizers by electrostatic layer-by-layer assembly and a series of post-treatments toward efficient quantum dot-sensitized mesoporous TiO2 solar cells. *Langmuir*, *28*(12), 5417-5426.

[89] Xi, Q., Chen, X., Evans, D. G., & Yang, W. (2012). Gold nanoparticle-embedded porous graphene thin films fabricated via layer-by-layer self-assembly and subsequent thermal annealing for electrochemical sensing.*Langmuir*, *28*(25), 9885-9892.

[90] Yan, Y., Björnmalm, M., & Caruso, F. (2013). Assembly of layer-by-layer particles and their interactions with biological systems. *Chemistry of Materials*, *26*(1), 452-460.

[91] Kim, Y., Kook, K., Hwang, S. K., Park, C., & Cho, J. (2014). Polymer/perovskite-Type nanoparticle multilayers with multi electric properties prepared from ligand addition-induced layer-By-layer assembly.*Acs Nano*, *8*(3), 2419-2430.

[92] Lvov, Y., Ariga, K., Ichinose, I., & Kunitake, T. (1995). Assembly of multicomponent protein films by means of electrostatic layer-by-layer adsorption. *Journal of the American Chemical Society*, *117*(22), 6117-6123.

[93] Linford, M. R., Auch, M., & Möhwald, H. (1998). Nonmonotonic effect of ionic strength on surface dye extraction during dye-polyelectrolyte multilayer formation. *Journal of the American Chemical Society*, *120*(1), 178-182.

[94] Zhang, Y., & Cao, W. (2001). Self-assembly of small molecules: An approach combining electrostatic self-assembly technology with host–guest chemistry. *New Journal of Chemistry*, *25*(3), 483-486.

[95] Baba, A., Park, M. K., Advincula, R. C., & Knoll, W. (2002). Simultaneous surface plasmon optical and electrochemical investigation of layer-by-layer self-assembled conducting ultrathin polymer films. *Langmuir*, *18*(12), 4648-4652.

[96] Constantine, C. A., Mello, S. V., Dupont, A., Cao, X., Santos, D., Oliveira, O. N., ... & Leblanc, R. M. (2003). Layer-by-layer self-assembled chitosan/poly (thiophene-3-acetic acid) and organophosphorus hydrolase multilayers. *Journal of the American Chemical Society*, *125*(7), 1805-1809.

[97] Serizawa, T., Kawanishi, N., & Akashi, M. (2003). Layer-by-Layer Assembly between Poly (vinylamine hydrochloride-co-N-vinylformamide) with Variable Primary Amine Content and Poly (sodium styrenesulfonate).*Macromolecules*, *36*(6), 1967-1974.

[98] Quinn, J. F., & Caruso, F. (2004). Facile tailoring of film morphology and release properties using layer-by-layer assembly of thermoresponsive materials. *Langmuir*, *20*(1), 20-22.

[99] Croll, T. I., O'Connor, A. J., Stevens, G. W., & Cooper-White, J. J. (2006). A blank slate? Layer-by-layer deposition of hyaluronic acid and chitosan onto various surfaces. *Biomacromolecules*, *7*(5), 1610-1622.

[100] Stricker, J. T., Gudmundsdóttir, A. D., Smith, A. P., Taylor, B. E., & Dursock, M. F. (2007). Fabrication of organic thin-film transistors using layer-by-layer assembly. *The journal*

of Physical Chemistry B, 111(23), 6322-6326.

[101] Lee, S. W., Kim, B. S., Chen, S., Shao-Horn, Y., & Hammond, P. T. (2008). Layer-by-layer assembly of all carbon nanotube ultrathin films for electrochemical applications. *Journal of the American Chemical Society, 131*(2), 671-679.

[102] Crouzier, T., & Picart, C. (2009). Ion pairing and hydration in polyelectrolyte multilayer films containing polysaccharides. *Biomacromolecules, 10*(2), 433-442.

[103] Martins, G. V., Mano, J. F., & Alves, N. M. (2010). Nanostructured self-assembled films containing chitosan fabricated at neutral pH. *Carbohydrate Polymers*, *80*(2), 570-573.

[104] Martins, G. V., Merino, E. G., Mano, J. F., & Alves, N. M. (2010). Crosslink Effect and Albumin Adsorption onto Chitosan/Alginate Multilayered Systems: An in situ QCM – D Study. *Macromolecular Bioscience, 10*(12), 1444-1455.

[105] Martins, G. V., Mano, J. F., & Alves, N. M. (2011). Dual responsive nanostructured surfaces for biomedical applications. *Langmuir*, *27*(13), 8415-8423.

[106] Qi, Z. D., Saito, T., Fan, Y., & Isogai, A. (2012). Multifunctional coating films by layer-by-layer deposition of cellulose and chitin nanofibrils.*Biomacromolecules*, *13*(2), 553-558.

[107] Cook, M. T., Tzortzis, G., Khutoryanskiy, V. V., & Charalampopoulos, D. (2013). Layer-by-layer coating of alginate matrices with chitosan–alginate for the improved survival and targeted delivery of probiotic bacteria after oral administration. *Journal of Materials Chemistry B*, *1*(1), 52-60.

[108] Oliveira, S. M., Silva, T. H., Reis, R. L., & Mano, J. F. (2013). Nanocoatings contraining sulfated polysaccharides prepared by layer-by-layer assembly as models to study cell-material interactions. *Journal of Materials Chemistry B, 1*(35), 4406-4418.

[109] Gomes, A. P., Mano, J. F., Queiroz, J. A., & Gouveia, I. C. (2013). Layer-by-layer deposition of antimicrobial polymers on cellulosic fibers: a new strategy to develop bioactive textiles. *Polymers for Advanced Technologies, 24*(11), 1005-1010.

[110] Leite, Á. J., Sher, P., & Mano, J. F. (2014). Chitosan/chondroitin sulfate multilayers as supports for calcium phosphate biomineralization. *Materials Letters*, *121*, 62-65.

[111] Hua, F., Cui, T., & Lvov, Y. M. (2004). Ultrathin cantilevers based on polymer-ceramic nanocomposite assembled through layer-by-layer adsorption. *Nano Letters*, *4*(5), 823-825.

[112] Yang, Y. H., Malek, F. A., & Grunlan, J. C. (2010). Influence of deposition time on layer-by-layer growth of clay-based thin films. *Industrial & Engineering Chemistry Research*, *49*(18), 8501-8509.

[113] Zhuk, A., Mirza, R., & Sukhishvili, S. (2011). Multiresponsive clay-containing layer-by-layer films. *Acs Nano, 5*(11), 8790-8799.

[114] Ichinose, I., Senzu, H., & Kunitake, T. (1996). Stepwise Adsorption of Metal Alkoxides on Hydrolyzed Surfaces: A Surface Sol-Gel Process. *Chemistry letters*, (10), 831-832.

[115] Ichinose, I., Senzu, H., & Kunitake, T. (1997). A surface sol-gel process of TiO2 and other metal oxide films with molecular precision. *Chemistry of materials*, *9*(6), 1296-1298.

[116] Ichinose, I., Kawakami, T., & Kunitake, T. (1998). Alternate Molecular Layers of Metal Oxides and Hydroxyl Polymers Prepared by the Surface Sol-Gel Process. *Advanced Materials, 10*(7), 535-539.

[117] Wang, Q., Zhong, L., Sun, J., & Shen, J. (2005). A facile layer-by-layer adsorption and reaction method to the preparation of titanium phosphate ultrathin films. *Chemistry of materials*, *17*(13), 3563-3569.

[118] Zebli, B., Susha, A. S., Sukhorukov, G. B., Rogach, A. L., & Parak, W. J. (2005). Magnetic targeting and cellular uptake of polymer microcapsules simultaneously functionalized with magnetic and luminescent nanocrystals.*Langmuir*, *21*(10), 4262-4265.

[119] Ai, S., He, Q., Tian, Y., & Li, J. (2007). Fabrication of mesoporous titanium oxide nanotubes based on layer-by-layer assembly. *Journal of nanoscience and nanotechnology*, *7*(7), 2534-2537.

[120] Jalil, R., & Nixon, J. R. (1990). Biodegradable poly (lactic acid) and poly (lactide-co-glycolide) microcapsules: problems associated with preparative techniques and release properties. *Journal of microencapsulation*, *7*(3), 297-325.

[121] Wu, X. S. (1995). Preparation, characterization, and drug delivery applications of microspheres based on biodegradable lactic/glycolic acid polymers. *Encyclopedic handbook of biomaterials and bioengineering*. New York: Marcel Dekker, 1151-1250.

[122] Arshady, R. (1991). Preparation of biodegradable microspheres and microcapsules: 2. Polyactides and related polyesters. *Journal of Controlled Release*, *17*(1), 1-21.

[123] Park, J. W., Hong, K., Kirpotin, D. B., Papahadjopoulos, D., & Benz, C. C. (1997). Immunoliposomes for cancer treatment. *Advances in pharmacology, 40*, 399-435.

[124] Moya, S., Donath, E., Sukhorukov, G. B., Auch, M., Bäumler, H., Lichtenfeld, H., & Möhwald, H. (2000). Lipid coating on polyelectrolyte surface modified colloidal particles and polyelectrolyte capsules.*Macromolecules*, *33*(12), 4538-4544.

[125] Noor Al-Naser.(2013). *Remote controlled drug release in drug-eluting stents*. University of Strathclyde.

[126] Abraham Samuel Finny.(2014). *Construction of Nano-Assembled Microcapsules Embedded with gold nanoparticles for use in novel drug delivery system*. University of Strathclyde.

[127] Ai, H., Jones, S. A., & Lvov, Y. M. (2003). Biomedical applications of electrostatic layer-by-layer nano-assembly of polymers, enzymes, and nanoparticles. *Cell biochemistry and biophysics*, *39*(1), 23-43.

[128] Jain, S., Hirst, D. G., & O'sullivan, J. M. (2014). Gold nanoparticles as novel agents for cancer therapy. *The British journal of radiology*.

[129] Huang, X., & El-Sayed, M. A. (2010). Gold nanoparticles: optical properties and implementations in cancer diagnosis and photothermal therapy. *Journal of Advanced Research*, *1*(1), 13-28.

[130] Radt, B., Smith, T. A., & Caruso, F. (2004). Optically addressable nanostructured capsules. *Advanced Materials, 16*(23-24), 2184-2189.

[131] Angelatos, A. S., Radt, B., & Caruso, F. (2005). Light-responsive polyelectrolyte/gold nanoparticle microcapsules. *The Journal of Physical Chemistry B*, *109*(7), 3071-3076.

[132] Skirtach, A. G., Antipov, A. A., Shchukin, D. G., & Sukhorukov, G. B. (2004). Remote activation of capsules containing Ag nanoparticles and IR dye by laser light. *Langmuir*, *20*(17), 6988-6992.

[133] Pavlov, A. M., Saez, V., Cobley, A., Graves, J., Sukhorukov, G. B., & Mason, T. J. (2011). Controlled protein release from microcapsules with composite shells using high frequency ultrasound—potential for *in vivo* medical use. *Soft Matter*, *7*(9), 4341-4347.

[134] Skrabalak, S. E., Chen, J., Sun, Y., Lu, X., Au, L., Cobley, C. M., & Xia, Y. (2008). Gold nanocages: synthesis, properties, and applications. *Accounts of Chemical Research*, *41*(12), 1587-1595.

[135] Yu, Y. Y., Chang, S. S., Lee, C. L., & Wang, C. C. (1997). Gold nanorods: electrochemical synthesis and optical properties. *The Journal of Physical Chemistry B*, *101*(34), 6661-6664.

[136] Shukla, R., Bansal, V., Chaudhary, M., Basu, A., Bhonde, R. R., & Sastry, M. (2005). Biocompatibility of gold nanoparticles and their endocytotic fate inside the cellular compartment: a microscopic overview. *Langmuir*, *21*(23), 10644-10654.

[137] Link, S., & El-Sayed, M. A. (2003). Optical properties and ultrafast dynamics of metallic nanocrystals. *Annual review of physical chemistry, 54*(1), 331-366.

[138] Underwood, S., & Mulvaney, P. (1994). Effect of the solution refractive index on the color of gold colloids. *Langmuir*, *10*(10), 3427-3430.

[139] Suppan, P. (1994). *Chemistry and light*. Royal Society of Chemistry.

[140] Mulvaney, P. (1996). Surface plasmon spectroscopy of nanosized metal particles. *Langmuir*, *12*(3), 788-800.

[141] Rae, J., Ashokkumar, M., Eulaerts, O., von Sonntag, C., Reisse, J., & Grieser, F. (2005). Estimation of ultrasound induced cavitation bubble temperatures in aqueous solutions. *Ultrasonics sonochemistry*, *12*(5), 325-329.

[142] El Fagui, A., Dalmas, F., Lorthioir, C., Wintgens, V., Volet, G., & Amiel, C. (2011). Well-defined core-shell nanoparticles containing cyclodextrin in the shell: a comprehensive study. *Polymer*, *52*(17), 3752-3761.

[143] Graham, T. (1861). Liquid diffusion applied to analysis. *Philosophical transaction of the Royal Society of London, 151*, 183-224.

[144] Parida, U. K., & Nayak, P. (2012). Biomedical Applications of Gold Nanoparticles: Opportunity and Challenges. *World Journal of Nano Science & Technology*, *1*(2), 10-25.

[145] Pavlov, A. M., Saez, V., Cobley, A., Graves, J., Sukhorukov, G. B., & Mason, T. J. (2011). Controlled protein release from microcapsules with composite shells using high frequency ultrasound—potential for *in vivo* medical use. *Soft Matter*, *7*(9), 4341-4347.

[146] Bastús, N. G., Comenge, J., & Puntes, V. (2011). Kinetically controlled seeded growth synthesis of citrate-stabilized gold nanoparticles of up to 200 nm: size focusing versus Ostwald ripening. *Langmuir*, *27*(17), 11098-11105.

[147] Zhu, F. Y., Wang, Q. Q., Zhang, X. S., Hu, W., Zhao, X., & Zhang, H. X. (2014). 3D nanostructure reconstruction based on the SEM imaging principle, and applications. *Nanotechnology*, *25*(18), 185705.

[148] Valeur, B., & Berberan-Santos, M. N. (2012). *Molecular fluorescence: principles and applications*. John Wiley & Sons.

[149] Lleres, D., Swift, S., & Lamond, A. I. (2007). Detecting protein-protein interactions *in vivo* with FRET using multiphoton fluorescence lifetime imaging microscopy (FLIM). *Current portocols in cytometry*, 12-10.

[150] Antipov, A. A., Sukhorukov, G. B., Donath, E., & Möhwald, H. (2001). Sustained release properties of polyelectrolyte multilayer capsules. *The Journal of Physical Chemistry B*, *105*(12), 2281-2284.

[151] López Arbeloa, F., Tapia Estévez, M. J., López Arbeloa, T., & Lopez Arbeloa, I. (1997). Spectroscopic rhodamine 6G study of the adsorption of on clay minerals in aqueous suspensions. *Clay Minerals*, *32*(1), 97-106.

[152] Arbeloa, F. L., Arbeloa, T. L., Lage, E. G., Arbeloa, I. L., & De Schryver, F. C. (1991). Photophysical properties of rhodamines with monoethylamino groups R19 and R6G in

water—ethanol mixtures. *Journal of Photochemistry and Photobiology A: Chemistry*, *56*(2), 313-321.

[153] Arbeloa, T. L., Estévez, M. T., Arbeloa, F. L., Aguirresacona, I. U., & Arbeloa, I. L. (1991). Luminescence properties of rhodamines in water/ethanol mixtures. *Journal of luminescence*, *48*, 400-404.

[154] Apfel, R. E., & Holland, C. K. (1991). Gauging the likelihood of cavitation from short-pulse, low-duty cycle diagnostic ultrasound. *Ultrasound in medicine & biology*, *17*(2), 179-185.

[155] Laugier, P., & Haïat, G. (2011). Introduction to the physics of ultrasound. In Bone quantitative ultrasound (pp. 29-45). Springer Netherlands.

[156] Pierce, A. D. (1981). Acoustics: an introduction to its physical principles and applications (Vol. 20). New York: McGraw-Hill.

[157] Kinsler, L. E., Frey, A. R., Coppens, A. B., & Sanders, J. V. (1999). Fundamentals of acoustics. Fundamentals of Acoustics, 4th Edition, by Lawrence E. Kinsler, Austin R. Frey, Alan B. Coppens, James V. Sanders, pp. 560. ISBN 0-471-84789-5. Wiley-VCH, December 1999., 560.

[158] Hall, D. E. (1987). Basic acoustics. Wiley.

[159] F. P. Schäfer (Ed.), *Dye Lasers*, 3rd Ed. (Springer-Verlag, Berlin, 1990).

[160] Duarte, F. J., Kelley, P., Hillman, L. W., & Liao, P. F. (1990). *Dye laser principles*. Academic Press.

[161] Kubin, R. F., & Fletcher, A. N. (1983). Fluorescence quantum yields of some rhodamine dyes. *Journal of Luminescence*, *27*(4), 455-462.

[162] Navarro, J. R., & Werts, M. H. (2013). Resonant light scattering spectroscopy of gold, silver and gold–silver alloy nanoparticles and optical detection in microfluidic channels. Analyst, 138(2), 583-592.

[163] El Fagui, A., Wintgens, V., Gaillet, C., Dubot, P., & Amiel, C. (2014). Layer-by-Layer Coated PLA Nanoparticles with Oppositely Charged β-Cyclodextrin Polymer for Controlled Delivery of Lipophilic Molecules. *Macromolecular Chemistry and Physics, 215*(6), 555-565.

[164] Mirkin, C. A., Letsinger, R. L., Mucic, R. C., & Storhoff, J. J. (1996). A DNA-based method for rationally assembling nanoparticles into macroscopic materials. *Nature*, *382*(6592), 607-609.

[165] Rae, J., Ashokkumar, M., Eulaerts, O., von Sonntag, C., Reisse, J., & Grieser, F. (2005). Estimation of ultrasound induced cavitation bubble temperatures in aqueous solutions. *Ultrasonics sonochemistry*, *12*(5), 325-329.

[166] Shchukin, D. G., Gorin, D. A., & Möhwald, H. (2006). Ultrasonically induced opening of polyelectrolyte microcontainers. *Langmuir*, *22*(17), 7400-7404.

[167] Skirtach, A. G., De Geest, B. G., Mamedov, A., Antipov, A. A., Kotov, N. A., & Sukhorukov, G. B. (2007). Ultrasound stimulated release and catalysis using polyelectrolyte multilayer capsules. *Journal of meterials chemistry, 17*(11), 1050-1054.

[168] De Geest, B. G., Skirtach, A. G., Mamedov, A. A., Antipov, A. A., Kotov, N. A., De Smedt, S. C., & Sukhorukov, G. B. (2007). Ultrasound-Triggered Release from Multilayered Capsules. *Small, 3*(5), 804-808.

[169] Kolesnikova, T. A., Gorin, D. A., Fernandes, P., Kessel, S., Khomutov, G. B., Fery, A., ... & Möhwald, H. (2010). Nanocomposite microcontainers with high ultrasound

sensitivity. *Advanced Functional Materials*, *20*(7), 1189-1195.

[170] Rübe, A., Hause, G., Mäder, K., & Kohlbrecher, J. (2005). Core-shell structure of Miglyol/poly (d, l-lactide)/Poloxamer nanocapsules studied by small-angle neutron scattering. *Journal of controlled release*, *107*(2), 244-252.

[171] Poletto, F. S., Jäger, E., Cruz, L., Pohlmann, A. R., & Guterres, S. S. (2008). The effect of polymeric wall on the permeability of drug-loaded nanocapsules. *Materials Science and Engineering: C*, *28*(4), 472-478.

[172] Radtchenko, I. L., Sukhorukov, G. B., & Möhwald, H. (2002). Incorporation of macromolecules into polyelectrolyte micro-and nanocapsules via surface controlled precipitation on colloidal particles. *Colloids and Surfaces A: Physicochemical and Engineering Aspects*, *202*(2), 127-133.

[173] Agarwal, A., Lvov, Y., Sawant, R., & Torchilin, V. (2008). Stable nanocolloids of poorly soluble drugs with high drug content prepared using the combination of sonication and layer-by-layer technology. *Journal of Controlled Release*, *128*(3), 255-260.

[174] Balakrishnan, B., Dooley, J. F., Kopia, G., & Edelman, E. R. (2007). Intravascular drug release kinetics dictate arterial drug deposition, retention, and distribution. *Journal of Controlled Release*, *123*(2), 100-108.

[175] Hoare, T., Timko, B. P., Santamaria, J., Goya, G. F., Irusta, S., Lau, S., ... & Kohane, D. S. (2011). Magnetically triggered nanocomposite membranes: a versatile platform for triggered drug release. *Nano letters*, *11*(3), 1395-1400.

[176] Dubreuil, F., Shchukin, D. G., Sukhorukov, G. B., & Fery, A. (2004). Polyelectrolyte capsules modified with YF3 nanoparticles: an AFM study.*Macromolecular rapid communications*, *25*(11), 1078-1081.

[177] Skirtach, A. G., Dejugnat, C., Braun, D., Susha, A. S., Rogach, A. L., Parak, W. J., ... & Sukhorukov, G. B. (2005). The role of metal nanoparticles in remote release of encapsulated materials. *Nano letters*, *5*(7), 1371-1377.

[178] Kolesnikova, T. A., Khlebtsov, B. N., Shchukin, D. G., & Gorin, D. A. (2008). Atomic force microscopy characterization of ultrasound-sensitive nanocomposite microcapsules. *Nanotechnologies in Russia*, *3*(9-10), 560-569.